Ab Initio Quantum Chemical and Experimental (Shock Tube) Studies of the Pyrolysis Kinetics of Acetonitrile

Karina Sendt, Emi Ikeda,‡ George B. Bacskay, and John C. Mackie*

School of Chemistry, University of Sydney, NSW 2006, Australia

Received: August 26, 1998; In Final Form: December 1, 1998

The pyrolysis kinetics of acetonitrile dilute in argon has been studied in the temperature range 1400−2100 K at an average pressure of 12 atm in single-pulse shock tube experiments. The principal products are HCN, C_2H_2, CH_4, and H_2, while the minor products include HCCCN, H_2CCHCN, C_2H_4, and C_4H_2. The overall kinetics is successfully simulated by an 87 step kinetic model that accurately accounts for the temperature profiles of the major products and also provides an acceptable fit for the minor products. The thermochemistry and rate parameters of a number of key reactions have been obtained by ab initio quantum chemical calculations carried out at CASSCF, CASPT2, and Gaussian-2 levels of theory. Several distinct reaction pathways were studied, whereby the geometries, vibrational frequencies, and energies of approximately 70 molecular species representing reactants, products, intermediates, and transition states were computed. The pyrolysis of acetonitrile is initiated by CH bond fission, forming a cyanomethyl radical. This reaction is the most sensitive one in the kinetic model. On the basis of sensitivity analyses of the model as well as ab initio calculations, the heat of formation of cyanomethyl has been revised as $\Delta_f H^0_{298}(CH_2CN) = 263 \pm 9$ kJ mol^{-1}. The limiting high-pressure value of the corresponding rate constant, as obtained by ab initio variational transition state calculations, is $k_{1\infty} = 1.2 \times 10^{16} \exp(-413 \text{ kJ mol}^{-1}/RT)$ s^{-1}, which is in good agreement with our extrapolated experimental measurement. A number of the observed products, including HCCCN and H_2CCHCN, largely arise from the decomposition of succinonitrile, a key intermediate, that forms by the recombination of two cyanomethyl radicals.

Introduction

To reduce the emission of pollutant oxides of nitrogen (NO_x) from the large-scale burning of coal and other nitrogen-containing fuel, an important strategy is to use staged combustion involving a primary reaction zone that is fuel-rich.[1] Most fuel-bound nitrogen in coals of varying rank is found in five-membered pyrrolic ring structures and in six-membered pyridinic structures. Fuel-rich combustion of these heterocyclic structures takes place initially essentially as pyrolysis in which volatile nitrogen-containing precursors of NO_x such as HCN and acetonitrile are evolved and undergo complex oxidative processes eventually to form NO and other products of oxidation. It is through initial rapid pyrolysis of the volatile precursors that radical species are produced for subsequent oxidation reactions. Thus, a detailed understanding of the pyrolysis of a model precursor such as acetonitrile, CH_3CN, is of importance for unravelling the subsequent oxidative reaction pathways leading to NO.

The pyrolysis of CH_3CN was investigated some years ago by Lifshitz, Moran, and Bidani[2] using single pulse shock tube techniques at temperatures between 1350 and 1950 K and at pressures around 3 atm. They showed that HCN and acetylene were principal products of the pyrolysis initiated through CH fission to produce the cyanomethyl, CH_2CN, radical. Lifshitz et al. also observed additional products including acrylonitrile, H_2CCHCN, and cyanoacetylene, HCCCN, thought to arise from combination of two CH_2CN radicals. Although they reported a value for the rate constant for the reaction $CH_3CN \rightarrow CH_2CN + H$, Lifshitz et al. did not carry out detailed kinetic modeling of the pyrolysis. More recently, Ikeda and Mackie[3] presented a detailed kinetic model for the fuel-rich oxidation of acetonitrile. Their oxidation model contained an acetonitrile pyrolysis model as a subset. This subset contained several pyrolysis reactions, not sensitive under oxidative conditions, that warrant further investigation. In a more recent study, Lifshitz, Tamburu, and Carroll[4] presented a kinetic model for the ignition delay in mixtures of acetonitrile and oxygen in argon.

The observation of significant amounts of H_2CCHCN and HCCCN in the products is intriguing since Lifshitz et al.[2] did not report any formation of the expected product of recombination of two CH_2CN radicals, viz., succinonitrile, $NCCH_2CH_2CN$, even at quite low reaction temperatures. Evidently, this molecule should be an intermediate and it must decompose in an unexpectedly facile way to produce acrylonitrile and cyanoacetylene. Thus, because of the importance of the pyrolysis mechanism in the understanding of oxidation of organonitriles, a further investigation of the pyrolysis of acetonitrile and the development of a detailed reaction mechanism is warranted. Furthermore, a study of the electronic structure and reactions of CH_2CN is of importance in its own right, since cyanomethyl is the simplest nitrile analogue of the important CH_3 radical and it is of interest to understand the effect of CN substitution on the electronic properties of a simple alkyl radical.

The present work involves an experimental shock tube kinetic study of the pyrolysis kinetics of acetonitrile dilute in argon over the temperature range 1400−2100 K at an average pressure of 12 atm and residence times of the order of 0.8 ms, together with an ab initio quantum chemical investigation of several key elementary reactions in the pyrolysis. In particular, we report

* Corresponding author. E-mail: j.mackie@chem.usyd.edu.au. FAX: +61-2-9351-3329.

‡ Present address: Department of Chemical Engineering, University of Illinois at Chicago, Chicago IL 60607.

10.1021/jp9835216 CCC: $18.00
Published on Web 02/05/1999

ab initio derived rate constants for the initiation reaction and for hydrogen atom addition to acetonitrile and a detailed investigation of the succinonitrile potential energy surface and of possible routes to acrylonitrile and cyanoacetylene. From the experimental data and the ab initio calculations we derive a detailed kinetic model of the pyrolysis of acetonitrile.

While this manuscript was under preparation, Lifshitz and Tamburu[5] published a modeling study of their earlier acetonitrile pyrolysis data.[2] The rate constants presented in their kinetic model, in contrast with our work, were optimized to fit their experimental product profiles, rather than derived on the basis of ab initio calculations. Consequently, it is instructive to compare several of our theoretically rate derived constants with those presented in their model.

Experimental Section

The principal reactor used in this study is the single-pulse shock tube. The shock tube has been used previously to study the pyrolyses of coal model compounds such as pyrrole[6] and the butenenitriles.[7] The temperature range covered in the present study was 1400−2100 K over the pressure range 10−14 atm with a residence time behind the reflected shock front between 700 and 1000 μs.

Some experiments were also carried out in a fused silica jet-stirred reactor that has been described previously.[8] The well-stirred nature of this reactor was established in earlier studies of the pyrolysis of cyclopropane.[8,9] Samples such as acetonitrile that are liquid at room temperature are injected by means of a syringe pump into a vaporizing oven where the vapor is mixed with a metered stream of argon from a mass flow controller. The reaction mixture then flows into the jet-stirred reactor, which is mounted inside an electrical furnace. When operated at pressures around 100 Torr and a residence time of 1 s, the reactor well approximates a completely stirred reactor (CSTR). This reactor is equipped with tandem cold traps and is useful for studying trace products of reaction. Reactions of acetonitrile and succinonitrile dilute in argon have been studied in the CSTR over the temperature ranges of 1240−1320 K for acetonitrile and 670−970 K for succinonitrile, respectively. Succinonitrile is a solid at room temperature but is readily soluble in acetonitrile. Acetonitrile solutions of succinonitrile were injected into the CSTR after vaporization and dilution of the vapor with argon. Succinonitrile decomposed over a temperature range below the onset of decomposition of acetonitrile itself; hence the former can be studied without significant interference from acetonitrile. A further advantage of acetonitrile as a solvent for succinonitrile as opposed to, e.g., a hydrocarbon solvent is that cyanomethyl radicals arising from CC fission in succinonitrile will merely be regenerated if they undergo hydrogen abstraction reactions with acetonitrile, thus minimizing secondary product formation and enabling us to search for possible intramolecular routes to acrylonitrile and HCN.

In the shock tube studies, reactant mixtures were prepared dilute in argon. The acetonitrile concentration was 0.4% in argon. Acetonitrile (Waters Associates, HPLC Grade, >99%) was thoroughly degassed and used without further purification. There was no detectable impurity by GC. In the CSTR studies, the total reactant concentration (either pure acetonitrile or succonitrile/acetonitrile mixture) in the vapor phase was 4% in argon. Solutions of succinonitrile in acetonitrile were 13 mol %.

Analyses of the reactant mixture and products in the shock tube experiments were carried out using an on-line Hewlett-Packard 5890II GC, equipped with a HP1 capillary column and detection by FID and a nitrogen phosphorus detector (NPD). In the flow reactor studies, reactants and volatile products were analyzed using the same gas chromatograph. In the CSTR experiments condensable products were extracted from the cold traps using dichloromethane and the extracts analyzed by GC. Some scatter in the chromatograms of cyanoacetylene occurred. Separation of this species from acetonitrile was troublesome at low levels of CH_3CN because the acetonitrile peak eluted on the leading edge of the cyanoacetylene peak. This led to integration problems when the residual acetonitrile was low and the yield of HCCCN high, causing some scatter in the recorded cyanoacetylene yields. Light hydrocarbons were analyzed with a Shimadzu GC-9A with an alumina column and FID. A sample of the product mixture was taken in a gastight syringe for hydrogen analysis using a Shimadzu GC-8A with TCD.

Product identification was made by means of GC/MS using a Hewlett-Packard MS Engine also using a 5890II GC and HP1 column, and where possible, confirmed by retention time matching with authentic samples. When these were not available, the online NBS MS library NBS 54K was used.

Theoretical and Computational Methods

The potential energy surfaces (PES) of the reactions were studied by using ab initio quantum chemical methods, computing the geometries, energies, and vibrational frequencies of the appropriate species that correspond to stationary points, viz. equilibrium and transition state geometries. For those systems where a single reference expansion of the wave function is valid, the Gaussian-2 (G2) method[10] was used. For singlet biradical species and a number of transition states that were found to display an appreciable degree of near-degeneracy, the geometries and vibrational frequencies were obtained using the complete active space (CASSCF) method[11,12] in conjunction with Dunning's[13] double-ζ plus polarization functions (DZP) basis. A given CASSCF calculation with *nel* active electrons in an active space of *nao* orbitals will be denoted CASSCF(*nel*/*nao*). In this work, depending on the system, these multiconfigurational SCF calculations range from CASSCF(3/4) to CASSCF(10/10).

When applied to larger systems, such as the decomposition reactions of succinonitrile and acrylonitrile, the G2 method was modified so as to make these calculations feasible on our smaller workstations. First, in the modified method, the ΔE(2df) correction is made at the MP2 level of theory (instead of MP4). Second, the MP2/6-311+G(3df,2p) energy is estimated as

$$E(\text{MP2/6-311+G(3df,2p)}) \approx E(\text{MP2/6-311G(3df,2p)}) + E(\text{MP2/6-311+G(2df,p)}) - E(\text{MP2/6-311G(2df,p)}) \quad \text{(i)}$$

When tested for a few of the smaller systems studied here, the results obtained by this modified G2 theory were found to be very close to the G2 results, the average difference in the calculated energies being ~3 kJ mol^{-1}.

Given that the wave functions in the G2 method are based on single reference expansions, G2 cannot be used to describe singlet biradical systems. On the other hand, contrary to our initial expectations that it would run into difficulties for transition states with an appreciable degree of near-degeneracy, G2 was found to perform well in the calculation of most transition state energies.

In the study of the decomposition reactions of succinonitrile, the energies were also computed at the CASPT2[14,15] level of theory (at CASSCF/DZP geometries) using the cc-pVDZ basis set[16,17] of Dunning. In these calculations the reference states range from CASSCF(6/6) to CASSCF(10/10). For selected pathways the energies were also calculated at the CASPT2 level

of theory with a CASSCF(10/10) reference in conjunction with the cc-pVTZ basis set,[17] but with the 4f and 3d polarization functions removed from the heavy and H atoms, respectively, resulting in a valence triple-ζ basis with two sets of polarization functions: VTZ2P.

Agreement between the G2 and CASPT2 relative energies is generally found to be good for species with the same spin state, although CASPT2 theory appears to have consistently predicted the singlet/triplet separations in carbenes to be ~30 kJ mol^{-1} larger than the corresponding G2 values. The results of studies on smaller carbenes (:CH_2, :CF_2, and :CHF), where the theoretical values could be compared with experiment, also conform to this trend. The comparisons with experimental values indicate, however, that G2 underestimates the relative stability of triplet molecules by ~10 kJ mol^{-1} while CASPT2 tends to overestimate it by ~20 kJ mol^{-1}. By contrast, multireference configuration interaction (MRCI) calculations, which were also carried out on these small molecules as a further check, using the same basis set as in the CASPT2 studies, yielded results in close agreement with experiment. Interestingly, however, MRCI and CASPT2 gave very similar results in a calculation of the lowest singlet → triplet vertical excitation energy of ethylene, both underestimating it by ~20 kJ mol^{-1}. By comparison, the G2 value of 431 kJ mol^{-1} is an overestimate by 10 kJ mol^{-1}. A similar level of disagreement between CASPT2 and G2 to that noted above was also found to occur when computing the dissociation energy of a formally closed shell singlet state molecule to doublet state fragments.

In the study of the decomposition reactions of acrylonitrile, where in addition to G2, energies were also calculated at the CASPT2 level of theory (at CASSCF geometries) with eight active electrons in eight orbitals using the cc-pVDZ basis set, the agreement between the G2 and CASPT2 relative energies has been found to be generally poorer than for the succinonitrile. For these reactions the CASPT2 results for intermediates, transition states, and products relative to acrylonitrile are systematically ~15 kJ mol^{-1} higher than the G2 results. Using the larger VTZ2P basis as well as the larger (10/10) active space, the above discrepancy between CASPT2 and G2 has been reduced to 11 kJ mol^{-1}. However, if we compare the CASPT2 and QCISD(T) energies obtained using the same VTZ2P basis, the difference becomes just 6.6 kJ mol^{-1}. We may thus conclude that much of the discrepancy between CASPT2/cc-pVDZ and G2 noted above is the result of a combination of factors, such as the obvious differences in basis sets as well as the choice of active space in the CASPT2 calculations.

Rate constants and Arrhenius rate parameters for the reactions of interest were calculated using the appropriate computed energies and partition functions according to Transition State Theory.[18] The partition functions of the various species were calculated from the ab initio data, using the standard formulas for classical rigid rotors, translations, and with the exception of molecules with low vibrational frequencies, quantum harmonic oscillators.[19] (Thermal corrections to enthalpies, as well as molecular entropies and specific heats were also obtained from these partition functions.) Certain low-frequency modes, when identified as torsional modes, were treated separately as hindered rotors,[19] whereby their contribution to the partition functions were calculated from the computed energy levels of individual one-dimensional rotors. The latter were obtained by solving the appropriate Schrödinger equation, using the generalized finite element method,[20] for a one-dimensional rotor in the presence of potential generated by a series of pointwise ab initio energy calculations.

In the case of simple bond fission reactions where there is no energy barrier along the reaction coordinate, i.e., no saddle point on the potential energy surface, the rate constants were obtained using Variational Transition State Theory.[21] This entails the computation of the rate constant along the reaction coordinate and locating its minimum, which then defines the transition state. For the CH bond fission reactions in our work the walk along the reaction coordinate was performed by starting with a geometry that is essentially that of the product, but with a CH bond distance of 2.0 Å. Allowing for a series of Newton−Raphson relaxations with a small trust radius, i.e., small steps, so as to search for a saddle point, then results in a walk on the potential energy surface that is effectively along the reaction coordinate. At each step then the rate constant was calculated at a range of temperatures, from which data the variational rate constant at each temperature of interest is readily obtained. All rate constants were calculated in the temperature range 1400−2100 K and fitted to an Arrhenius form in order to obtain the appropriate activation energies and frequency, viz. *A* factors, in this temperature range.

Many of the reactions are expected to be in the falloff regime at our average experimental pressure of 12 atm. For pressure dependent reactions, RRKM calculations have been carried out using the UNIMOL program.[22] In this treatment, molecular vibration frequencies have been considered to be harmonic. Two of the external rotations are regarded as adiabatic with the third rotational degree of freedom (corresponding to the *K* rotational quantum number) considered to be active. Hindered rotors, where identified, have been considered explicitly. Unless otherwise specified, all falloff calculations have been made using a constant value of $\langle \Delta E_{down} \rangle$ of 500 cm^{-1}. Molecular parameters for reactant and transition state have been obtained by ab initio calculation.

For reactions that might proceed via chemical activation (e.g., addition of H to acetonitrile and subsequent fission), the possible stabilization of an intermediate adduct was investigated by QRRK analysis.[23,24] Barriers and high-pressure rate constants were taken from our ab initio calculations. The QRRK method uses a modified strong collision model for the energy transfer parameter, β, and a single geometric mean frequency for the adduct.[23]

The ab initio computations were carried out using the Gaussian-92,[25] Gaussian-94,[26] CADPAC 5.2,[27] CADPAC 6.0,[28] SIRIUS,[29] ABACUS,[30] DALTON,[31] MOLCAS-2,[32] MOLCAS-4,[33] and MOLPRO[34] packages on DEC alpha and IBM RS2000 workstations.

Results and Discussion

Product Distribution. The principal products of the shock tube pyrolysis of acetonitrile are HCN, C_2H_2, CH_4, and H_2. There are lesser amounts of HCCCN, H_2CCHCN, and C_4H_2. At very low extents of decomposition, yields of CH_4 and HCN are approximately equal. Distributions of products were similar to those reported by Lifshitz et al.[2] Small yields of cyanogen, dicyanomethane, ethyl cyanide, *cis*- and *trans*-fumaronitrile, dicyanoacetylene, C_2 and C_3 hydrocarbons, and benzene were also detected in the present study. Profiles of the reactant and major pyrolysis products are shown in Figure 1. We have been unable to detect any succinonitrile in our shock tube pyrolyses although we have observed succinonitrile in acetonitrile pyrolysis in our jet-stirred reactor at lower temperatures (~1300 K and 1 s residence time). The lack of detection in the shock tube experiments results either because succinonitrile has low volatility or because it was formed but decomposed very rapidly.

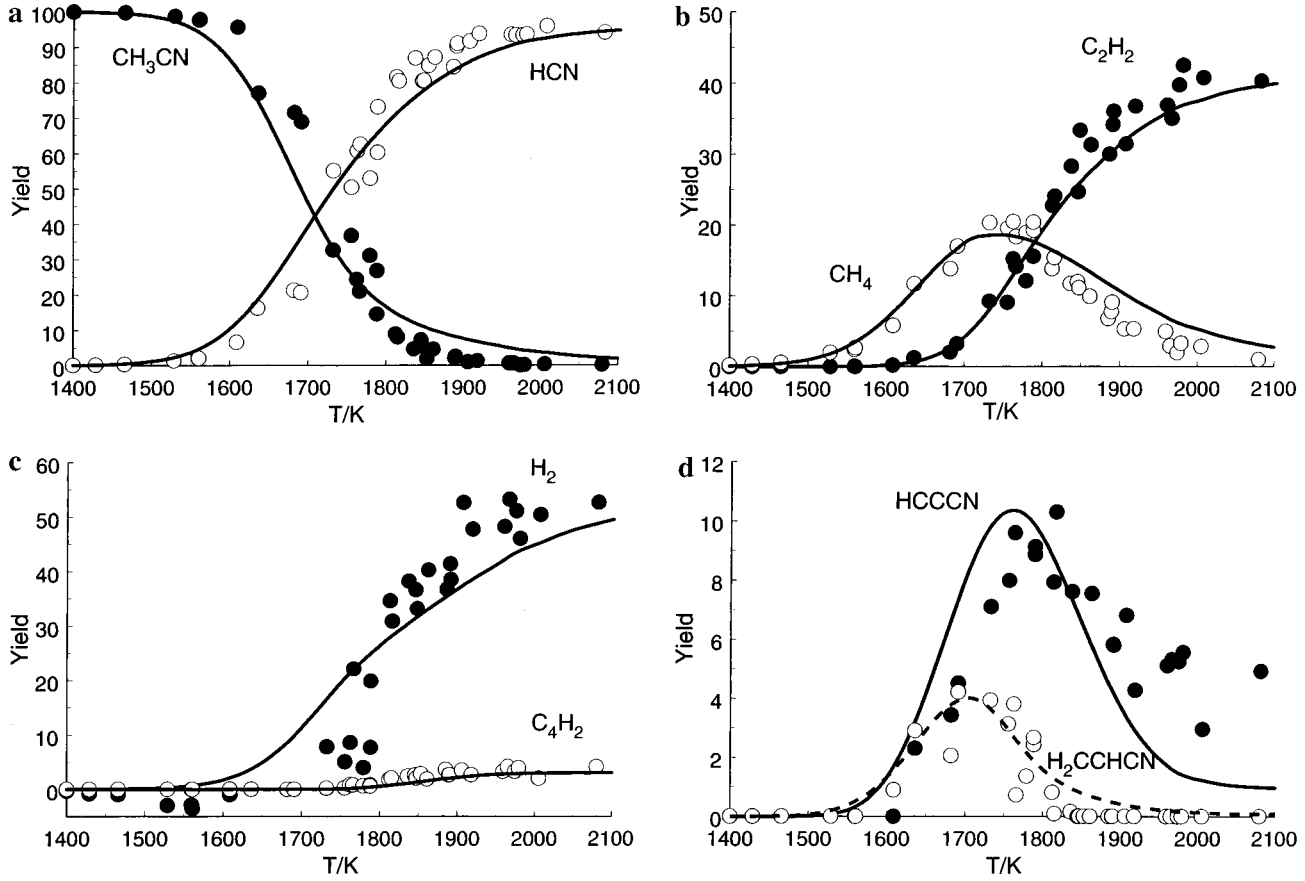

Figure 1. Temperature dependence of yield (%) of designated species in the pyrolysis of acetonitrile. Symbols = data points, lines = model prediction.

However, because elemental mass balances of reactant and product were generally achieved within 10% and there was no systematic mass loss with increase in pyrolysis temperature, we consider that a significant yield of succinonitrile could not have been formed and, additionally, we have been able to detect the rather involatile products *cis*- and *trans*-fumaronitrile, albeit in low yield.

In the jet-stirred reactor at a temperature of 1300 K and residence time of 1 s, acetonitrile underwent significant decomposition. Major products were similar to those observed in the shock tube experiments. Additionally, extracts from the cold traps revealed the presence of trace amounts of dicyanomethane, the fumaronitriles, dicyanoacetylene, and as mentioned above, traces of succinonitrile, identified by GC/MS.

Succinonitrile vapor (in the presence of acetonitrile vapor) started to decompose at 700 K (1 s residence time). At temperatures below ~900 K the only products detected were HCN and acrylonitrile. Low Arrhenius parameters typical of surface-enhanced reaction were measured for this reaction in the CSTR. Above 900 K other products including ethyl cyanide and the fumaronitriles were also detected.

Kinetics of Disappearance of CH_3CN. Thermochemical considerations (see below) lead to the conclusion that the only feasible initiation reaction is CH fission to produce the cyanomethyl radical:

$$CH_3CN \rightarrow H + CH_2CN \qquad (1)$$

An Arrhenius plot for the rate constant for disappearance of acetonitrile (behind the reflected shock front) is shown in Figure 2. This plot shows considerable curvature at values of $1/T < 5.7 \times 10^{-4}$ K^{-1}. Part of this curvature results from falloff in the rate constant k_1 at higher temperatures. The participation of secondary reactions would also lead to marked non-Arrhenius behavior. Approximate Arrhenius parameters for the disappearance of CH_3CN were $A = 10^{14.6\pm0.3}$ s^{-1} and $E_a = 397$ kJ mol^{-1}, estimated from the data in Figure 2 by considering only values of ln k_{dis} at values of $1/T > 5.7 \times 10^{-4}$ K^{-1}.

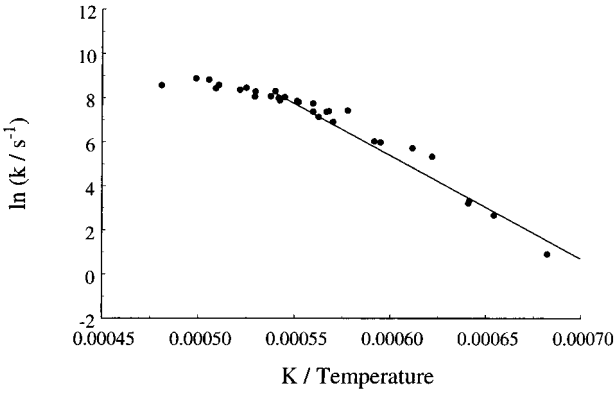

Figure 2. Arrhenius plot for the rate constant for disappearance of acetonitrile.

Although the apparent rate constant should be less influenced by secondary reactions over this range of temperatures, the participation of these reactions is still likely to have a significant influence of the rate of disappearance of acetonitrile. At best we can only obtain from the experimental Arrhenius plot an initial estimate of the Arrhenius parameters for k_1, the rate constant for the decomposition reaction 1. When proper allowance is made for secondary reactions in the kinetic modeling to be described below, a more accurate rate constant for k_1 will be derived. It is expected that this value, for a pressure of ~12

atm, would be in the falloff regime. However, before considering the extrapolation of our rate data to the high-pressure limit, it is instructive to consider the results of the ab initio calculations on the various isomers of CH_2CN, and especially the enthalpy of formation of cyanomethyl, which is the most stable C_2H_2N isomer.

Computational Results

In the course of this work a total of ~70 molecular species, corresponding to reactants, products, intermediates, and transition states, were studied using ab initio methods. Apart from a few small molecules such as hydrogen cyanide, methane, acetylene, etc., no existing literature data of sufficient accuracy could be found for these species, hence the need for the current study on at least 65 of them. The computed MP2 and/or CASSCF geometries of these 65 species are given in Table 1S in the Supporting Information, while the Supporting Tables 2S−9S contain the corresponding absolute and relative QCISD(T), G2, and CASPT2 energies, respectively, as well as the computed zero point energies. In the paper itself the reaction energies and critical energies will be given in the form of molecular potential energy diagrams in the appropriate sections. These diagrams also show schematic structures of the various molecular species along with a number (**1**−**65**) that had been assigned to each distinct molecule. Unless indicated otherwise, the relative energies quoted in these diagrams and used in the computation of reaction energies and Arrhenius are from G2 calculations of the electronic energies at MP2 or CASSCF geometries, as indicated in Table 1S. All vibrational frequencies were scaled by 0.8929, when computing zero point energies and other thermodynamic quantities.

Thermochemistry of CH_3CN. The enthalpy of formation of acetonitrile (**1**) was calculated from the following (isogyric and isodesmic) pathways:

$$CH_3CN + H_2 \rightarrow CH_4 + HCN$$

$$CH_3CN + CH_4 \rightarrow C_2H_6 + HCN$$

From the computed G2 enthalpies of the reactants and products (at 298 K), the heats of the above reactions, $\Delta_r H^0_{298}$, were obtained. Using the latter, in conjunction with the experimental values for the $\Delta_f H^0_{298}$ of H_2, CH_4, HCN, and C_2H_6 (taken from the CHEMKIN thermodynamic database[35]), the heat of formation, $\Delta_f H^0_{298}$, of acetonitrile was computed to be 79.1 kJ mol^{-1}. This is slightly higher than the value of 73.9 ± 0.8 kJ mol^{-1} that had been previously derived on the basis of experimental kinetic data.[36]

On thermochemical grounds, the first step in the decomposition of acetonitrile is the cleavage of the CH bond, resulting in the formation of the cyanomethyl radical and atomic hydrogen. (Other possible initiation channels, such as fission to CH_3 + CN, elimination of HCN to form CH_2 or elimination of H_2 to form HCCN, can be discounted because of their high heats of reaction. Furthermore, the elimination reactions would also be expected to have barriers in addition to their unfavorably high reaction enthalpies.) The enthalpy of formation of the cyanomethyl radical (**2**) was calculated by utilizing the G2 value of $\Delta_f H^0_{298}$ of the isodesmic reaction:

$$CH_3CN + CH_3 \rightarrow CH_4 + CH_2CN$$

The resulting $\Delta_f H^0_{298}$ of cyanomethyl is then 267 kJ mol^{-1}, when the G2 value is used for $\Delta_f H^0_{298}$ of acetonitrile. If the above experimental value is used for the latter, we obtain 261 kJ mol^{-1} as the $\Delta_f H^0_{298}$ of cyanomethyl. These values are significantly higher than the previously reported value of 245 ± 9 kJ mol^{-1}, obtained from pyrolysis kinetics of alkanenitriles.[37] In recent times there have been claims[38] that the derivation of heats of formation from pyrolysis kinetics could lead to systematic errors of the order of 8 kJ mol^{-1}. Indeed, a higher value of 250 ± 8 kJ mol^{-1} has been obtained by Moran et al.[39] on the basis of the observed electron and proton affinities of cyanomethyl and the $\Delta_f H^0_{298}$ of acetonitrile. Substituting our computed value of 79.1 kJ mol^{-1} for the latter would yield 255 ± 8 kJ mol^{-1} as $\Delta_f H^0_{298}(CH_2CN)$. However, on the basis of the ab initio results our conservative estimate for $\Delta_f H^0_{298}(CH_2CN)$ is 263 ± 9 kJ mol^{-1}, which overlaps the upper bounds of the experimental values. The kinetic modeling described in a later section leads to computed species profiles of reactant and all major products that agree significantly better with experiment if the higher value of $\Delta_f H^0_{298}(CH_2CN)$, viz. 263 kJ mol^{-1}, is used.

The heat of reaction at 298 K for the first step is thus 405 kJ mol^{-1} when computed on the basis of the theoretical heats of formation of acetonitrile and cyanomethyl (and the experimental heat of formation of atomic hydrogen). Direct calculation of the energetics of the fission reaction yields a heat of reaction of 410 kJ mol^{-1}, indicating that the various theoretical approaches are consistent and any error cancelations in the isodesmic or isogyric schemes are small.

The rate constants for this fission reaction at a range of temperatures were estimated using variational transition state theory with a PES calculated at the CASSCF(6/6)/DZP level of theory. The energy was scaled so as to make the CASSCF dissociation energy consistent with the value of 405 kJ mol^{-1} for the heat of reaction at 298 K. In the temperature range 1400−2100K, the transition state (structure **3** in Table 1S) was found to have a CH bond length of approximately 2.5 Å, which contracts slightly as the temperature is increased. Such a contraction has been also noted in the dissociation of methane.[21] Using the calculated rate constants, which correspond to transition states with different bond lengths at different temperatures, yielded an A factor of 1.2×10^{16} s^{-1} and an activation energy of 411 kJ mol^{-1} when an Arrhenius fit of the rate constants was carried out. The Arrhenius parameters used in the kinetic modeling are 8.0×10^{14} s^{-1} and 397 kJ mol^{-1}, specific to the 12 atm pressure of the experiments. (The falloff calculation of the rate constant is discussed in the section on Kinetic Modeling.)

C_2H_2N Potential Energy Surface. The C_2H_2N PES was studied in order to ascertain whether there are any low lying isomers of the cyanomethyl radical that may need to be considered in the kinetic modeling, especially since the mass spectrometric and thermochemical studies of Holmes and Mayer[40] suggested the possible presence of a low-energy cyclic isomer. In our study five isomers were located as local minima on the PES. Their structures and relative energies are summarized in Table 1. Note, however, that the valence structures of these isomers as drawn (as well as those of many other species to be discussed later) are only meant to provide a qualitative guide to the bonding. Thus, e.g., the Lewis structure of the isocyanomethyl radical CH_2NC implies the presence of formal charges on the cyanide C and N atoms, while the molecular orbital (MO) calculations suggest a CN triple bond between atoms that are effectively neutral.

As expected, cyanomethyl is the most stable isomer, viz., global minimum on the PES. In comparison with acetonitrile, cyanomethyl was found to have a shorter CN bond as well as

TABLE 1: Isomers of C_2H_2N: Structures, Energies (Relative to Cyanomethyl), Symmetries, and Spectroscopic States

Molecule	Structure	Energy /kJ mol^{-1}	Symmetry	State
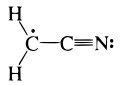	**2**	0	C_{2v}	$^2B_1$
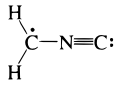	**4**	102	C_{2v}	$^2B_1$
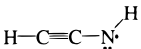	**5**	130	C_s	$^2A''$
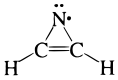	**6**	220	C_{2v}	$^2B_1$
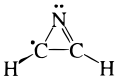	**7**	227	C_1	^2A

a considerably shorter CC bond (1.412 Å), indicating that a greater degree of π delocalization that includes the unpaired electron is present in the radical. Isocyanomethyl and the ketene iminyl radical (structures **4** and **5**) are found to be the lowest energy isomers of cyanomethyl. As one may expect, the energy difference of 102 kJ mol^{-1} between CH_2NC and CH_2CN is comparable with the corresponding G2 value of 98 kJ mol^{-1} that was computed for the parent molecules CH_3NC and CH_3-CN. The relatively high stability of the ketene iminyl radical can be similarly attributed to the high degree of π bonding, viz., delocalization. The length of the CC triple bond was found to be 1.227 Å, slightly longer than the accepted standard value for a triple bond, viz. 1.20 Å. However, the CN bond length was found to be 1.272 Å, which is comparable with the experimental and computed C═N distances in CH_2NH[41] that range from 1.27 to 1.28 Å, while being only slightly longer than the CN distance of 1.228 Å that had been computed for ketene imine.[42] This suggests that there is substantial π delocalization across the CCN moiety with the participation of the nonbonding electrons of nitrogen. The two cyclic structures (**6**, **7**) are, however, considerably less stable than the open chain isomers, owing to the presence of σ strain as well as the weaker π bonds. The situation is thus qualitatively different from that of the cationic species, where a cyclic isomer (with two π electrons) is formally aromatic and has been found to be the most stable, both experimentally[40] and computationally.[43] The above energetics suggest that isomerization reactions of the cyanomethyl radical are unlikely to be important reaction pathways.

After the initial submission of this manuscript a paper appeared by Mayer et al.[44] that includes an ab initio study of the thermochemistry of CH_3CN and three isomers of CH_2CN (structures **2**, **4**, and **7** of Table 1). Their computed heats of formation of these molecules are in excellent agreement with those reported in this work.

Decomposition Mechanism of CH_3CN. We expect that HCN principally arises from addition of H atoms to the reactant and subsequent fissioning of the adduct into HCN and CH_3 according to the complex process

$$H + CH_3CN \rightarrow CH_3C(H)N \rightarrow CH_3 + HCN \qquad (2a)$$

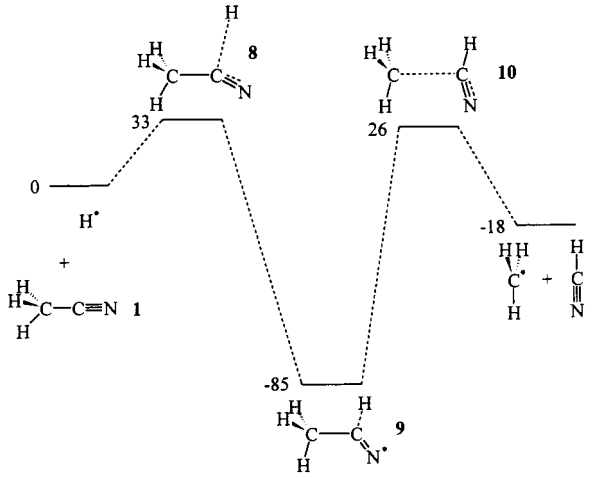

Figure 3. Potential energy surface for reaction between atomic hydrogen and acetonitrile. (Energies at 0 K given in kJ mol^{-1}.)

The PES for these reactions is shown in Figure 3. The attack by a hydrogen atom at the nitrile carbon results in a fairly stable intermediate (**9**). The transition state (**8**) associated with this reaction has a critical energy of 33 kJ mol^{-1} at 0 K. It is characterized by a long HC bond of length 1.74 Å and a CCN angle of 154.8°. The $CH_3C(H)N$ intermediate (**9**) has a CN bond length of 1.226 Å, which is consistent with a CN double bond, as are the bond angles of ∼120° around the nitrile C atom. The unpaired electron is largely localized on the N atom. The subsequent CC bond cleavage via a transition state (**10**), where the CC distance is 2.147 Å, results in a methyl radical and hydrogen cyanide as products. This second transition state was found to lie 26 kJ mol^{-1} above the reactants at 0 K and the overall reaction was found to be exothermic by 18 kJ mol^{-1}. The calculated A factor of 5.3×10^{14} cm^3 mol^{-1} s^{-1} and activation energy of 51 kJ mol^{-1} (in the temperature range 1400−2100 K) are the parameters that were computed for the first (slow) step. The ab initio potential energy surface for reaction 2a has been used in conjunction with a QRRK analysis to show that under our experimental conditions the intermediate adduct is not stabilized. Thus, in the development of the detailed kinetic mechanism given in Table 2 (discussed in the section on Kinetic Modeling), reaction 2 represents the overall addition and fission process and the rate constant given in Table 2 is the result of the QRRK analysis using the computed ab initio data. The reactions where a hydrogen attack occurs at the nitrogen atom were found to result in intermediates (trans and cis), which are approximately 33 and 55 kJ mol^{-1} higher in energy (at 0 K), respectively, than the intermediate (**9**) in the carbon attack pathway discussed above.

Other reactions important in the mechanism involve abstraction by H and CH_3 radicals, and rate constants for these reactions shown in Table 2 have been also evaluated in the present study. The cyanomethyl radical plays an important role in the mechanism, along with CH_3, CN, and H, as evidenced by the observed termination products that include ethyl cyanide, dicyanomethane, and cyanogen.

Recombination Reaction of Cyanomethyl Radicals. In agreement with previous work by Lifshitz et al.[2] we have observed in our shock tube studies significant yields of cyanoacetylene and acrylonitrile without observing any succinonitrile, viz., the dimer of cyanomethyl, $NCCH_2—CH_2CN$. Lifshitz et al. suggested that two CH_2CN radicals recombine to form a $C_4H_4N_2$ intermediate, which then decomposes to acrylonitrile and HCN, which are among the observed products. Thermochemical calculations, however, suggest that if this

TABLE 2: Kinetic Model for Acetonitrile Pyrolysis

		forward rate constant			reverse rate constant			
	reactions[a]	log A[b]	n	E_a/kJ mol^{-1}	log A	n	E_a/kJ mol^{-1}	ref
1	$CH_3CN \leftrightarrow CH_2CN + H$	14.90	0.00	397.5	12.96	0.00	−10.5	PW[c,d]
2	$H + CH_3CN \leftrightarrow CH_3 + HCN$	14.00	0.00	40.5	12.65	0.00	62.5	PW/QRRK[c]
3	$H + CH_3CN \leftrightarrow CH_2CN + H_2$	13.18	0.00	41.8	11.85	0.00	71.0	PW
4	$CH_3 + CH_3CN \leftrightarrow CH_2CN + CH_4$	12.70	0.00	29.3	12.79	0.00	59.5	PW
5	$CN + CH_3CN \leftrightarrow HCN + CH_2CN$	13.70	0.00	8.4	12.80	0.00	110.8	est[c]
6	$CN + CH_3CN \leftrightarrow CH_3 + C_2N_2$	13.00	0.00	41.8	12.95	0.00	88.9	est
7	$2CH_2CN \leftrightarrow SUCC$	13.36	0.00	0.0	16.71	0.00	308.8	PW
8	$2CH_2CN \rightarrow HCN + H_2CCHCN$	27.92	−3.95	184.9	0.00	0.00	0.0	PW/QRRK
9	$SUCC \leftrightarrow H_2CCHCN + HCN$[e]	14.46	0.00	366.1	12.84	0.00	268.6	PW/abin[c]
10	$SUCC \leftrightarrow ISUCC$	14.34	0.00	260.0	14.39	0.00	187.1	PW/abin
11	$ISUCC \leftrightarrow H_2CCHCN + HCN$	14.77	0.00	334.7	13.10	0.00	310.2	PW/abin
12	$SUCC \leftrightarrow NCCHCH_2CN + H$	15.40	0.00	400.4	13.49	0.00	−0.2	PW/abin
13	$H + SUCC \leftrightarrow H_2 + NCCHCH_2CN$	13.48	0.00	20.9	12.19	0.00	57.5	est
14	$H + SUCC \leftrightarrow CH_2CH_2CN + HCN$	14.30	0.00	41.8	13.04	0.00	93.6	est
15	$CH_3 + SUCC \leftrightarrow CH_4 + NCCHCH_2CN$	12.30	0.00	20.9	12.43	0.00	58.5	est
16	$CN + SUCC \leftrightarrow HCN + NCCHCH_2CN$	13.70	0.00	8.4	12.84	0.00	118.2	est
17	$CH_2CN + SUCC \leftrightarrow CH_3CN + NCCHCH_2CN$	12.54	0.00	20.9	12.58	0.00	28.3	est
18	$NCCHCH_2CN \leftrightarrow H_2CCHCN + CN$	14.34	0.00	230.1	13.58	0.00	22.8	PW/abin
19	$NCCHCH_2CN \leftrightarrow H + C_4H_2N_2$	13.75	0.00	198.7	14.86	0.00	33.9	PW/abin
20	$CH_2CH_2CN \leftrightarrow H_2CCHCN + H$	13.49	0.00	153.1	13.14	0.00	3.8	est
21	$CH_3 + CH_2CN \leftrightarrow C_2H_5CN$	13.30	0.00	0.0	16.10	0.00	339.7	est
22	$CN + CH_2CN \leftrightarrow NCCH_2CN$	13.00	0.00	0.0	15.85	0.00	412.5	est
23	$CH_3CN \leftrightarrow CH_3 + CN$	15.00	0.00	489.5	12.61	0.00	1.1	est
24	$HCCHCN \leftrightarrow HCCCN + H$	12.00	0.00	196.6	12.80	0.00	7.6	7
25	$H + HCCHCN \leftrightarrow H_2CCHCN$	13.60	0.00	0.0	15.39	0.00	440.0	7
26	$H + H_2CCHCN \leftrightarrow HCN + C_2H_3$	12.70	0.00	33.5	10.98	0.00	13.4	PW
27	$H + H_2CCHCN \leftrightarrow HCCHCN + H_2$	13.70	0.00	33.5	12.53	0.00	30.6	7
28	$H_2CCHCN \leftrightarrow HCCCN + H_2$	12.24	0.19	318.0	12.56	0.00	128.7	PW[d]
29	$H_2CCHCN \leftrightarrow C_2H_2 + HCN$	12.42	0.13	318.0	11.37	0.00	155.1	PW[d]
30	$C_4H_4 \leftrightarrow 2C_2H_2$	15.17	0.00	345.2	13.84	0.00	194.8	59
31	$C_4H_4 \leftrightarrow C_4H_2 + H_2$	14.30	0.00	364.0	13.39	0.00	192.2	59
32	$C_2H_5 (+M) \leftrightarrow C_2H_4 + H (+M)$	13.30	0.00	166.0	12.57	0.00	10.2	53
33	$C_2H_4 + M \leftrightarrow C_2H_2 + H_2 + M$	17.41	0.00	331.8	15.92	0.00	160.0	53
34	$C_2H_4 + M \leftrightarrow C_2H_3 + H + M$	17.41	0.00	404.0	15.11	0.00	−60.2	53
35	$C_2H_4 + H \leftrightarrow C_2H_3 + H_2$	13.70	0.00	33.5	12.02	0.00	6.4	60
36	$H + C_2H_2 (+M) \leftrightarrow C_2H_3 (+M)$	13.00	0.00	11.3	12.81	0.00	156.0	61,57[g]
37	$2CH_3 (+M) \leftrightarrow C_2H_6 (+M)$	13.56	0.00	0.0	16.71	0.00	360.4	53
38	$C_2H_6 + H \leftrightarrow H_2 + C_2H_5$	2.73	3.50	21.8	14.88	0.00	99.6	54
39	$C_2H_6 + CH_3 \leftrightarrow CH_4 + C_2H_5$	−0.26	4.00	34.7	15.15	0.00	120.7	54
40	$CH_3 + H_2 \leftrightarrow CH_4 + H$	2.81	3.00	32.2	15.24	0.00	75.9	53
41	$HCCHCN \leftrightarrow C_2H_2 + CN$	13.70	0.00	242.7	12.92	0.00	7.5	est
42	$CN + H_2 \leftrightarrow HCN + H$	5.69	2.44	8.9	15.07	0.00	116.8	54
43	$C_2N_2 + M \leftrightarrow 2CN + M$	68.1	−13.22	715.9	17.28	0.00	−7.4	62
44	$H + C_2N_2 \leftrightarrow HCN + CN$	14.49	0.00	32.9	13.20	0.00	7.9	est
45	$CH_3 + H (+M) \leftrightarrow CH_4 (+M)$	16.78	−1.00	0.0	15.15	0.00	424.0	54
46	$2CH_2CN \leftrightarrow CH_3CN + NCCH(3)$	12.30	0.00	83.7	14.31	0.00	68.4	est
47	$C_2H_5 + H \leftrightarrow 2CH_3$	14.00	0.00	0.0	12.16	0.00	48.7	54
48	$H_2 + C_2H \leftrightarrow C_2H_2 + H$	5.61	2.39	3.6	15.05	0.00	120.5	52
49	$C_2H_3 + H \leftrightarrow C_2H_2 + H_2$	13.60	0.00	0.0	14.41	0.00	292.5	54
50	$C_2H + C_2H_2 \leftrightarrow C_4H_2 + H$	13.48	0.00	0.0	14.56	0.00	61.5	52
51	$2C_2H_2 \leftrightarrow C_4H_3 + H$	12.30	0.00	192.0	11.74	0.00	−63.2	52
52	$C_4H_3 + M \leftrightarrow C_4H_2 + H + M$	16.00	0.00	249.8	16.35	0.00	46.5	52
53	$C_2H_2 + M \leftrightarrow C_2H + H + M$	16.62	0.00	447.7	15.33	0.00	−72.4	52
54	$2H + M \leftrightarrow H_2 + M$	18.00	−1.00	0.0	14.95	0.00	423.0	52
55	$2H + H_2 \leftrightarrow 2H_2$	16.96	−0.60	0.0	15.38	0.00	428.7	52
56	$CN + C_2H_3 \leftrightarrow H_2CCHCN$	13.80	0.00	0.0	16.56	0.00	530.5	est
57	$CH_2CH_2CN \leftrightarrow C_2H_4 + CN$	13.00	0.00	251.0	12.19	0.00	35.5	est
58	$H_2CCHCN + H \leftrightarrow CH_3CHCN$	13.00	0.00	19.7	13.59	0.00	193.6	est
59	$CH_3CHCN \leftrightarrow CH_3 + NCCH(3)$	13.00	0.00	376.6	11.35	0.00	−1.8	est
60	$H_2CCHCN + C_2H_3 \leftrightarrow HCCHCN + C_2H_4$	14.00	0.00	33.5	14.51	0.00	57.7	est
61	$2HCCHCN \leftrightarrow H_2CCHCN + HCCCN$	50.00	−10.5	284.5	14.06	0.00	86.4	est/QRRK
62	$C_2H_5CN \leftrightarrow H + CH_2CH_2CN$	15.00	0.00	410.0	13.69	0.00	1.0	est
63	$C_2H_5CN \leftrightarrow H + CH_3CHCN$	15.48	0.00	384.9	14.40	0.00	0.4	est
64	$C_2H_5CN + H \leftrightarrow H_2 + CH_2CH_2CN$	13.80	0.00	29.3	13.11	0.00	57.4	est
65	$C_2H_5CN + H \leftrightarrow H_2 + CH_3CHCN$	13.80	0.00	27.6	13.34	0.00	80.2	est
66	$C_2H_5CN + H \leftrightarrow HCN + C_2H_5$	14.00	0.00	41.8	13.64	0.00	83.5	est
67	$C_2H_5CN + CH_3 \leftrightarrow CH_4 + CH_2CH_2CN$	12.00	0.00	33.5	12.73	0.00	62.6	est
68	$C_2H_5CN + CH_3 \leftrightarrow CH_4 + CH_3CHCN$	12.00	0.00	33.5	12.96	0.00	87.1	est
69	$CH_2CN + C_2H_5CN \leftrightarrow CH_3CN + CH_2CH_2CN$	13.00	0.00	96.2	13.63	0.00	95.1	est
70	$CH_2CN + C_2H_5CN \leftrightarrow CH_3CN + CH_3CHCN$	13.00	0.00	117.2	13.87	0.00	140.6	est
71	$CH_2CN + C_2H_6 \leftrightarrow CH_3CN + C_2H_5$	13.00	0.00	41.8	13.63	0.00	40.8	est
72	$CH_2CN + M \leftrightarrow H_2 + C_2N + M$	15.00	0.00	418.4	13.77	0.00	86.8	est

TABLE 2 (Continued)

	reactions[a]	forward rate constant log A^b	n	E_a/kJ mol^{-1}	reverse rate constant log A	n	E_a/kJ mol^{-1}	ref
73	$CH_2CN \leftrightarrow H + NCCH(3)$	23.74	−3.09	434.5	12.45	0.00	−32.7	est[d]
74	$2NCCH(3) \leftrightarrow C_4H_2N_2$	13.00	0.00	0.0	15.43	0.00	589.9	est
75	$2C_2N \leftrightarrow C_4N_2$	12.70	0.00	0.0	16.72	0.00	653.8	est
76	$CN + C_2H_2 \leftrightarrow HCCCN + H$	11.70	0.00	0.0	13.28	0.00	46.1	est
77	$C_4H_2N_2 + H \leftrightarrow HCCHCN + HCN$	13.00	0.00	8.4	10.39	0.00	36.3	est
78	$SUCC \leftrightarrow c\text{-}C_4H_4N_2$	15.30	0.00	351.5	15.00	0.00	181.2	PW/abin
79	$c\text{-}C_4H_4N_2 \rightarrow H_2CCHCN + HCN$	15.48	0.00	246.9	0.00	0.00	0.0	PW/abin
80	$2CH_2CN \rightarrow HCN + H_2CCHCN$[f]	13.30	0.00	142.3	0.00	0.00	0.0	PW/abin
81	$CN + C_2H_2 \leftrightarrow HCN + C_2H$	13.70	0.00	20.9	13.46	0.00	11.3	est
82	$C_4H_2N_2 \leftrightarrow HCCCN + HCN$	13.70	0.00	309.6	11.89	0.00	148.5	PW[d]
83	$CN + HCCHCN \leftrightarrow C_4H_2N_2$	13.48	0.00	0.0	17.14	0.00	482.5	est
84	$HCN + M \leftrightarrow H + CN + M$	29.02	−3.30	529.7	15.86	0.00	−27.6	52
85	$H + CH_2CN \leftrightarrow NCCH(3) + H_2$	13.70	0.00	33.5	14.38	0.00	47.4	est
86	$CN + CH_2CN \leftrightarrow NCCH(3) + HCN$	13.70	0.00	8.4	14.81	0.00	95.5	est
87	$CH_3 + C_2H_2 \leftrightarrow C_2H + CH_4$	11.26	0.00	71.1	12.01	0.00	−10.8	62

[a] ↔ denotes reversible reaction, ⇒ denotes unidirectional reaction. (M) denotes a reaction in the falloff region; falloff parameters are given in the reference. [b] Units for A are cm^3 mol^{-1} s^{-1} or s^{-1} as appropriate. [c] PW denotes a rate constant determined in the present work. QRRK denotes that the value was obtained from QRRK analysis. est denotes a rate constant estimated in the present work. abin denotes a rate constant evaluated by ab initio calculation. [d] Value specific to the pressure of 12 atm. [e] Proceeds via 1,3 H-transfer. [f] Proceeds on triplet succinonitrile potential energy surface. [g] RRKM extrapolation by ref 57. SUCC: succinonitrile $NCCH_2CH_2CN$. $C_4H_2N_2$: *cis*- and *trans*-fumaronitrile. ISUCC: succinonitrile isocyanide $NCCH_2CH_2NC$. $c\text{-}C_4H_4N_2$:

intermediate is succinonitrile, it should be a stable intermediate whose energy is some 300 kJ mol^{-1} below that of two CH_2CN radicals. According to our calculations, cyanomethyl radicals can recombine by forming either a new CC bond giving succinonitrile (structure **11**) or a CN bonded isomer NC—CH_2—N=C=CH_2 (structure **12** in Table 1S). Preliminary calculations, however, indicated that succinonitrile was the more stable isomer by approximately 155 kJ mol^{-1}. Given this, as well as the fact that the observed products contain three to four carbon chains, as in succinonitrile, only reactions involving the latter molecule were further studied. Reaction 7, corresponding to the recombination of two cyanomethyl radicals to form succinonitrile, was calculated to be 317 kJ mol^{-1} exothermic at 0 K. The lowest triplet state of succinonitrile (structure **13** in Table 1S) was also investigated so as to determine whether the decomposition reactions of succinonitrile could occur on a triplet PES. As triplet succinonitrile was found to have an energy (at 0 K) that is 135 kJ mol^{-1} above that of two cyanomethyl radicals, the corresponding recombination reaction is unlikely to be important, even if its critical energy (not calculated in this work) is not significantly higher than the endothermicity. However, reaction 80, the direct reaction between two CH_2CN radicals on a triplet surface to form $H_2CCHCN + HCN$, was included in the kinetic model with an activation energy of 142 kJ mol^{-1}, which is based on an approximate barrier height of 135 kJ mol^{-1}. The sensitivity analysis that was carried out (see below) indicated that this direct mechanism had no sensitivity over the entire temperature range studied. The reaction involving the decomposition of succinonitrile to form acrylonitrile (structure **19**) and hydrogen cyanide was studied by exploring several different pathways.

Decomposition Reactions of Succinonitrile. The subsequent reactions of succinonitrile that are expected to yield the observed products acrylonitrile or cyanoacetylene must proceed via sufficiently low energy pathways in order to account for the significant quantities of these products as well as the fact that no significant amount of residual succinonitrile has been observed. Six different pathways were considered as chemically reasonable, and these were subsequently investigated in some detail by means of ab initio quantum chemical calculations. The pathways studied fall into three broad classes: (a) unimolecular rearrangement of succinonitrile followed by decomposition, (b) CH bond fission followed by decomposition of the resulting NC−CH_2−CH−CN radical, and (c) bimolecular abstraction of CN by a H atom, followed by decomposition of the resulting cyanoethyl radical.

1,3-Hydrogen Transfer Reaction. In this reaction scheme, the results of which are summarized in Figure 4a, a 1,3 type H-transfer takes place via a four-center transition state (**14**) to yield a biradical intermediate (**15**, **16**) followed by CC bond cleavage to yield acrylonitrile and HCN. The first transition state (**14**) is analogous to that calculated for the 1,3-H transfer in propene,[45] and indeed, the key geometric parameters of the two species are comparable. The computed critical energy of the H-transfer reaction is 352 kJ mol^{-1} at 0 K. The biradical species that results has a singlet ground state (**15**) although the corresponding triplet state (**16**) is quite close both structurally and energetically to the singlet, provided the energies are calculated at the same level of theory. Using CASPT2(10/10)/VTZ2P the singlet−triplet splitting was calculated to be −18 kJ mol^{-1}. As the triplet intermediate (**16**) was found to be 303 kJ mol^{-1} above succinonitrile at 0 K, the reaction that yields the singlet intermediate (**15**) is 285 kJ mol^{-1} endothermic at 0 K, when using the above estimate of singlet−triplet splitting. If the energy of this reaction is calculated directly from the CASPT2(10/10)/VTZ2P energies of both succinonitrile and the intermediate (**15**), the first step is predicted to be 256 kJ mol^{-1} endothermic. This difference arises largely from the discrepancy between the G2 and CASPT2 energies for triplet systems, as discussed in the section on Theoretical and Computational Methods. The A factor and activation energies for the first step were calculated to be 2.9×10^{14} s^{-1} and 366 kJ mol^{-1}, respectively, in the temperature range 1400−2100 K.

The singlet biradical (**15**) can undergo CC bond cleavage to produce HCN and ground-state acrylonitrile by passing through a transition state (**17**), whose geometry was optimized at the CASSCF(6/6) level. The CC distance of the breaking bond in the transition state was found to be ∼1.8 Å. Given that the

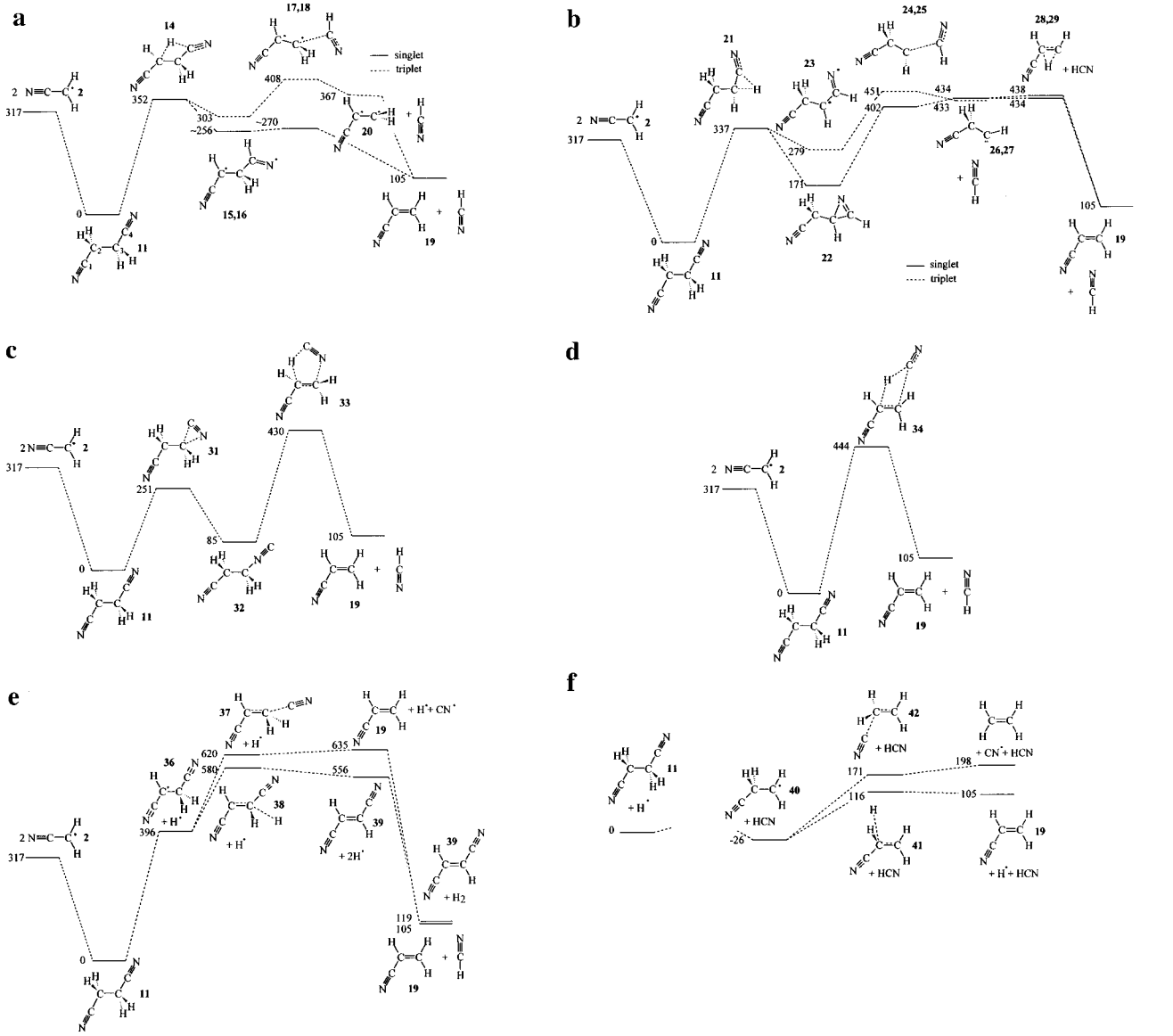

Figure 4. (a) Potential energy surface for decomposition of succinonitrile via 1,3-H migration. (Energies at 0 K given in kJ mol^{-1}.) (b) Potential energy surface for decomposition of succinonitrile via 1,2-H migration. (Energies at 0 K given in kJ mol^{-1}.) (c) Potential energy surface for decomposition of succinonitrile via an isocyanide intermediate. (Energies at 0 K given in kJ mol^{-1}.) (d) Potential energy surface for decomposition of succinonitrile via concerted elimination of HCN. (Energies at 0 K given in kJ mol^{-1}.) (e) Potential energy surface for decomposition of succinonitrile via CH bond fission. (Energies at 0 K given in kJ mol^{-1}.) (f) Potential energy surface for reaction between atomic hydrogen and succinonitrile. (Energies at 0 K given in kJ mol^{-1}.)

CASSCF wave function was found to be dominated by a single closed shell type configuration, the energy was initially computed using the G2 method, which predicts that the transition state (**17**) is 242 kJ mol^{-1} above succinonitrile, i.e., 43−14 kJ mol^{-1} below the intermediate (**15**), depending on the method used to estimate the energy of the singlet intermediate, suggesting that the bond breaking process may be barrierless. Of course, at the CASSCF(6/6) level (that had been used in the geometry optimizations) there is a barrier, albeit a very small one, with a height of 14 kJ mol^{-1}. Consequently, the barrier to CC bond cleavage on the singlet surface is unlikely to be significant. On the triplet surface, the transition state (**18**) that corresponds to CC bond cleavage is significantly higher in energy than the analogous singlet state and results in the formation of triplet acrylonitrile (**20**) and singlet HCN.

Acrylonitrile in its singlet state is planar, and on the basis of the computed bond lengths, such as the relatively short CC single bonds of 1.44−1.45 Å, it appears that there is a small degree of conjugation. The geometry in the triplet state is twisted but of C_s symmetry, and thus the electronic state is $^3A''$. The CC bond adjacent to the CN was found to be slightly shorter than in the singlet ground state, suggesting a comparable degree of conjugation. Interestingly, the CC bond linking the HCCN fragment to the methylene moiety was found to be only slightly longer at 1.46−1.48 Å. This is comparable with the CC distance of 1.456 Å in triplet ethylene (computed using the MP2/6-31G-(d) method, where the dihedral angle between the methylenes is 90°, but it is significantly shorter than the "normal" C−C bond length of ∼1.53 Å, e.g., in ethane.[41] The explanation for these short CC distances in these biradical species is in terms of hyperconjugation, viz., the stabilizing interaction of CH σ MO's with the half occupied p_π orbitals on the adjacent carbon atom(s). Singlet acrylonitrile and HCN were computed to be 105 kJ mol^{-1} above succinonitrile at 0 K. Although energetically triplet acrylonitrile (**20**) and HCN were found to lie 262 kJ mol^{-1} higher, this corresponds to an energy that is only 64 kJ mol^{-1} above the triplet intermediate (**16**). Intersystem crossing to the singlet surface is possible, either by spin−orbit coupling or via

a collisional mechanism; hence the reaction on the triplet surface could, in principle, be included in the kinetic model. However, given that on energetic considerations the singlet pathway appears to be substantially more favorable, the alternative pathway on the triplet PES is not part of our kinetic model. The kinetic parameters for reaction 9, viz., an *A* factor of 2.9×10^{14} s^{-1} and an activation energy of 366 kJ mol^{-1}, were thus derived on the basis of the 1,3-H transfer step (with a critical energy of 352 kJ mol^{-1}) being rate determining.

1,2-Hydrogen Transfer Reaction. In this reaction scheme, summarized in Figure 4b, a hydrogen atom migrates to the adjacent carbon atom of the cyano group of succinonitrile, followed by CC bond cleavage of the resulting cyclic or biradical intermediates (structures **22** and **23** respectively), resulting in HCN and 2-cyanoethylidene. A subsequent 1,2 hydrogen migration in the carbene yields acrylonitrile. The first transition state (structure **21**) lies 337 kJ mol^{-1} above succinonitrile at 0 K and its geometry is similar to those observed in studies of 1,2-H migration in propene.[45] Although the expected product of the initial 1,2-H transfer is a biradical, such a structure was found only for the triplet state (structure **23**). A singlet biradical structure could be obtained if it was constrained to have C_s symmetry, but at the CASSCF level such a structure is a saddle point with an imaginary frequency of $\sim$200 cm^{-1} corresponding to an a″ mode, indicating that the true equilibrium structure has lower symmetry. On removing the symmetry constraint the structure simply collapsed to a cyclic structure (structure **22**) with a formally closed shell electronic configuration. While the bond lengths and bond angles of this cyclic intermediate were found to be fairly insensitive to the method of optimization, the difference between the MP2 and CASSCF optimized dihedral angles is more substantial and this difference is possibly the main reason for the difference between the G2 and CASPT2 relative energies. The *A* factor and activation energies for this first step (reaction 78) were found to be 2.0×10^{15} s^{-1} and 353 kJ mol^{-1}, respectively, in the temperature range 1400−2100 K. The reverse reactions, viz., singlet intermediate to succinonitrile and triplet intermediate to succinonitrile, were found to have Arrhenius parameters of 1.6×10^{15} s^{-1} and 181 kJ mol^{-1} (reaction 78 in Table 2) and 4.7×10^{13} s^{-1} and 64 kJ mol^{-1}, respectively. Only the reaction pathway on the singlet PES was included in the modeling.

The second step in this reaction, involving CC bond cleavage to form HCN and a carbene was found to be considerably higher in energy than the corresponding step in the 1,3-hydrogen transfer pathway. The singlet transition state (structure **24**) was found to be 231 kJ mol^{-1} at 0 K above the singlet intermediate. Although the transition state resembles the CC bond cleavage of a singlet biradical system, geometry relaxation along the reverse pathway did in fact yield the closed shell ring structure. The triplet transition state (structure **25**) was found to be 172 kJ mol^{-1} above the triplet intermediate at 0 K. The geometries of the triplet and singlet transition states are quite similar, with the exception of the dihedral angle that specifies the relative orientation of the two fragments and, to a smaller extent, the CCH angle around the carbenic carbon, which is larger in the triplet, just as in methylene itself. The *A* factor and the activation energy of the singlet pathway (reaction 79) are 2.7×10^{15} s^{-1} and 248 kJ mol^{-1}, respectively, in the temperature range 1400−2100 K. For the triplet pathway, the corresponding values were found to be 3.3×10^{15} s^{-1} and 173 kJ mol^{-1}. Only the singlet pathway was considered in the kinetic modeling.

In the case of the singlet carbene intermediate (structure **26**) the G2 energies are such that it appears 30 kJ mol^{-1} less stable than the transition state leading to its formation, although at the CASSCF/DZP(6/6 and 10/10) levels of theory (which were used to optimize the geometries) the transition state is clearly higher in energy by 38−45 kJ mol^{-1}. This apparent contradiction is due to different levels of theory being used for the geometry optimization (CASSCF) and energy calculation (G2) for reactions with small barriers. The G2 calculations predict the singlet and triplet carbenes (structures **26** and **27**) as being effectively isoenergetic. Given the observation in the Theoretical and Computational Methods section that G2 tends to underestimate the singlet−triplet energy difference by $\sim$10 kJ mol^{-1}, a reasonable estimate of the latter quantity in these cyano carbenes is $\sim$11 kJ mol^{-1}.

To form singlet acrylonitrile, a 1,2-H migration in the singlet carbene is needed. Two transition states were found for such a migration. Structure **28** results when a hydrogen atom migrates so as to be trans to the cyano group. The structure is such that the migrating hydrogen is above the rest of the molecule, which is approximately planar. The barrier to this migration is just 1 kJ mol^{-1} at 0 K. The forward and reverse *A* factors and activation energies for this process in the temperature range 1400−2100 K were computed to be 3.6×10^{12} s^{-1}, 8.5×10^{13} s^{-1}, 3.5 kJ mol^{-1}, and 340 kJ mol^{-1}, respectively. Structure **29** is the transition state that results when a hydrogen atom migrates so as to be cis to the cyano group. This structure is qualitatively similar to **28**, apart from the obvious cis−trans difference, but it is associated with a slightly higher barrier, the difference being 4 kJ mol^{-1}. The forward and reverse *A* factors and activation energies in the temperature range 1400−2100 K are 3.3×10^{12} s^{-1}, 7.8×10^{13} s^{-1}, 7.3 kJ mol^{-1}, and 344 kJ mol^{-1}, respectively. Analogous calculations on the ethylidene molecule[46] have resulted in a critical energy of 3.3 kJ mol^{-1} for the singlet pathway at 0 K. These results suggest that the assumption that the singlet reaction goes to completion is valid. Therefore, in the kinetic modeling, the singlet carbene was not considered explicitly; instead, its decomposition to acrylonitrile was considered to be sufficiently fast and essentially irreversible so that reaction 79 was taken to correspond to the overall unidirectional formation of acrylonitrile and HCN.

The cyclic intermediate (**22**) discussed above and the biradical intermediate (**15**) of the 1,3-H migration pathway can, however, interconvert by a simple hydrogen migration that occurs via a three centered transition state (structure **30** in Table 1S). Energetically, this transition state was found to be 428 kJ mol^{-1} above succinonitrile and the *A* factor and activation energy for the **22** → **15** conversion were computed to be 5.4×10^{14} s^{-1} and 272 kJ mol^{-1}, respectively, while for the reverse reaction they are 1.2×10^{13} s^{-1} and 167 kJ mol^{-1} in the temperature range 1400−2100 K. This aspect of the potential energy surface was not considered in the kinetic modeling.

Rearrangement to Isocyanide. The reaction pathway involving an isocyanide isomer of succinonitrile as an intermediate is summarized in Figure 4c. Succinonitrile was expected and indeed found to be similar to acetonitrile in that it isomerizes readily to form an isocyanide, which then rearranges, yielding acrylonitrile and hydrogen cyanide as products. The transition state for the isomerization step (structure **31**) is very similar both structurally and energetically to that computed for acetonitrile.[42] The critical energy for this reaction was calculated as 251 kJ mol^{-1} at 0 K, with the reaction being 85 kJ mol^{-1} endothermic at this temperature. The *A* factor for the forward reaction (10) in the temperature range 1400−2100 K is 2.0×10^{14} s^{-1} and the corresponding activation energy is 260 kJ mol^{-1}. As each of the three species (**11**, **31**, **32**) in this first

reaction was found to have a low-frequency vibrational mode corresponding to hindered rotation about the central CC bond, the partition functions were also calculated using a hindered rotor approximation. However, the resulting *A* factors for the forward and reverse reactions hardly differed from those obtained by the all-vibrations model.

The second step in this pathway is a concerted elimination of HCN that occurs via a five-centered transition state (structure **33**). The geometry of this transition state is characterized by a very long breaking CN bond of length ~2.7 Å, as well as a long forming CH bond of length ~1.7 Å. The critical barrier for this reaction was computed to be 345 kJ mol^{-1} at 0 K. The resulting *A* factor and activation energy are 2.9×10^{15} s^{-1} and 364 kJ mol^{-1} respectively, in the temperature range 1400−2100 K (reaction 11).

Concerted Elimination of Hydrogen Cyanide. The details of the concerted elimination of hydrogen cyanide from succinonitrile are summarized in Figure 4d. This pathway is the simultaneous 1,3-H transfer and CC bond cleavage, and as such, it is associated with a single transition state (structure **34**) that is characterized by a very long forming CH bond of length ~1.8 Å, a long breaking CC bond of length ~2.5 Å, and a relatively short breaking CH bond of length ~1.247 Å. The HCN fragment in this transition state is near-linear (with an angle of 172.6°) and lies almost normal to the near-planar acrylonitrile fragment. The critical energy at 0 K for this reaction was found to be 444 kJ mol^{-1} at 0 K. In the temperature range 1400−2100 K, the *A* factor and activation energy were calculated to be 1.4×10^{16} s^{-1} and 463 kJ mol^{-1}, respectively. Preliminary modeling studies indicated that this reaction was far too slow to have a significant effect on the overall kinetics, and therefore, it has not been included in the final kinetic model.

CH Bond Fission Reaction. This mechanism, summarized in Figure 4e, is analogous to the CH bond fission in acetonitrile and in fact the endothermicities of the two reactions at 0 K are within 14 kJ mol^{-1} of each other. For a fission reaction such as this, where the reverse reaction is barrierless, variational transition state theory needs to be used in order to obtain kinetic parameters. The CASSCF calculations, similar to those performed on acetonitrile, were carried out using two different choices of active spaces: (6/6) and (10/10). The transition state structures that were located are effectively the same. The breaking CH bond distance in the transition state (structure **35**) is ~2.4 Å, nearly the same as for acetonitrile. The CH distance does depend on the temperature to some extent; it decreases with increasing temperature, as found for acetonitrile as well as methane.[21] To obtain the appropriate critical energy, the energies of reactant, transition state, and products were recalculated at the CASPT2(10/10)/cc-pVDZ level of theory and then scaled to bring the dissociation energy in line with the corresponding G2 energy. Since both succinonitrile and the transition state possess low-frequency modes (86 and 47 cm^{-1}, respectively) that correspond to hindered rotation about the central CC bond, the partition functions and hence rate constants were computed by the explicit hindered rotor treatment, as discussed in the Theoretical and Computational Methods section. The resulting *A* factor and activation energy in the temperature range 1400−2100 K are 1.4×10^{15} s^{-1} and 393 kJ mol^{-1}, respectively, when using the CASSCF(6/6)/DZP geometries and frequencies. The alternative all-vibrations model gave 2.5×10^{15} s^{-1} and 393 kJ mol^{-1}. Use of the CASSCF(10/10)/DZP geometries and frequencies in the all-vibrations model results in 7.2×10^{15} s^{-1} and 404 kJ mol^{-1}, indicating a fairly high level of sensitivity to the level of theory. Given that the vibrational frequency obtained for the hindered rotation in the transition state is lower than the analogous frequency in succinonitrile, one would expect that use of the hindered rotor treatment would have a larger effect on the partition function of the transition state than on that of succinonitrile. As expected, the partition functions of both systems increased when the above modes were treated as hindered rotors rather than harmonic vibrations, but the change turned out to be larger for succinonitrile, which then resulted in a lower *A* factor. The explanation of this unexpected trend is that while the rotational potential energy curves of both systems have three minima between 0 and 2π, in the transition state structure one of these minima occurs at too high an energy to contribute appreciably to the partition function, especially at lower temperatures. It is expected, however, that if the geometries were allowed to relax in conjunction with the internal rotation, the effect noted above would become less pronounced. The *A* factor and activation energy used in the kinetic model are 2.5×10^{15} s^{-1} and 400 kJ mol^{-1} (reaction 12).

The radical thus produced (structure **36**) can then decompose by further bond fission, with the loss of either a cyanide radical or of another H atom. The first of these reactions, yielding acrylonitrile and cyanide is endothermic by 239 kJ mol^{-1} at 0 K. Characterizing the transition state for this reaction proved elusive and we were unsuccessful in locating it using CASSCF theory. Thus, in this case the SCF geometry (structure **37**) is used instead, since SCF found a saddle point on the PES. The critical energy of this reaction was found to be 224 kJ mol^{-1} at 0 K. The energy of the transition state is actually lower than that of the products, when computed at a higher level of theory, which suggests that the barrier to the reverse reaction is likely to be quite small. Calculations on the chemically similar ethyl cyanide system (replacing −CN by −H), where both SCF and CASSCF successfully located the transition state, suggest that SCF theory is likely to underestimate by ~0.2 Å the length of the breaking CC bond, which was calculated to be 2.3 Å in structure **37**. Although the energetic effect of such a discrepancy is essentially negligible, it does have a more significant effect on the rotational constants, as well as on the computed frequencies, and hence on the partition function. Thus, in the ethyl cyanide reaction the *A* factor, calculated using the CASSCF geometry and frequencies, is 1.8 times larger than that obtained from the SCF geometry and frequencies. Nevertheless, in this work the kinetic parameters for reaction 18 are those based on the SCF structure and frequencies. The resulting *A* factor and activation energy are 2.2×10^{14} s^{-1} and 230 kJ mol^{-1}, respectively, in the temperature range 1400−2100 K.

With respect to the loss of H from radical **36**, there are two possible pathways leading to the formation of *cis*- or *trans*-dicyanoethylene. Only the second of these was studied. The transition state (structure **38**) was found to have a CH bond with a length of ~1.9 Å, with the leaving H atom out of plane with respect to the NCCCCN skeleton. The critical energy for this step was calculated to be 184 kJ mol^{-1} with an endothermicity of 160 kJ mol^{-1} at 0 K. The calculated *A* factor and activation energies in the temperature range 1400−2100 K were computed to be 5.6×10^{13} s^{-1} and 199 kJ mol^{-1}, and these parameters have been used in the kinetic modeling of reaction 19.

Loss of Cyanide Radical from Succinonitrile. Succinonitrile could lose a cyanide radical, resulting in a cyanoethyl radical (structure **41**) as a product. This step was found to be 505 kJ mol^{-1} endothermic at 0 K, and consequently, it is unlikely that this pathway could play a significant role in the decomposition

kinetics of succinonitrile since it is considerably more energetic than any of the other pathways. It is not included in the kinetic model and has not been studied further.

Bimolecular Reaction with Atomic Hydrogen. Atomic hydrogen could abstract a cyanide radical from succinonitrile in a way that is similar to the reaction (6) between acetonitrile and hydrogen. In this case the other product of the reaction is the cyanoethyl radical (structure **40**), which could then lose either a hydrogen atom to form acrylonitrile or a cyanide radical to form ethylene. These pathways are shown in Figure 4f. The first step in this reaction pathway is expected to have a low activation energy, as in the case of acetonitrile, and therefore it is unlikely to be rate determining. At 0 K, the first step was calculated to be 26 kJ mol^{-1} exothermic (cf. 18 kJ mol^{-1} for the acetonitrile reaction). This first step was not studied further computationally. The kinetic modeling parameters for the overall reaction (14) are an *A* factor of 2.0×10^{14} cm^3 mol^{-1} s^{-1} and an activation energy of 42 kJ mol^{-1}. Loss of hydrogen from cyanoethyl occurs via a transition state (structure **41**) with a breaking CH bond length of 1.65 Å, with the H atom above the plane of the acrylonitrile fragment. The critical energy for this reaction was computed to be 142 kJ mol^{-1} at 0 K with the corresponding *A* factor and activation energy being 3.1×10^{13} s^{-1} and 153 kJ mol^{-1} in the temperature range 1400−2100 K. These values have been used in the kinetic modeling (reaction 20).

Loss of CN from cyanoethyl is associated with a transition state (structure **42**) with a very long breaking CC bond of ∼2.6 Å, with the cyanide being above the plane of the ethylene fragment. The critical barrier for this reaction was found to be 197 kJ mol^{-1} at 0 K, with an *A* factor and activation energy of 1.8×10^{15} s^{-1} and 206 kJ mol^{-1}, respectively, in the temperature range 1400−2100 K. Although the energy of the transition state was found to lie below that of the products, at the CASSCF level of theory (that was used to optimize the geometry was carried out), the structure is unambiguously identifiable as a saddle point with an energy that is slightly higher than that of the products. Thus, it appears that the reverse barrier is quite low. Given that the computed value of 206 kJ mol^{-1} for the activation energy of reaction 57 is below the computed or experimental heats of reactions, in the kinetic model the activation energy for this reaction was increased to 251 kJ mol^{-1}. Sensitivity analysis (see Kinetic Modeling section) revealed, however, that reaction 57 was not a sensitive reaction.

Eliminations of H_2 and HCN from Acrylonitrile. Acrylonitrile, a cyano-substituted ethylene, can undergo decomposition in an analogous manner to ethylene. Quantum chemical studies[46] on the decomposition of ethylene revealed two decomposition pathways: first, loss of H_2 to form vinylidene followed by H-migration to form acetylene and, second, rearrangement to ethylidene followed by loss of H_2. The vinylidene pathway was found to be the lower energy route, and although a direct 1,2 elimination was searched for, no transition state corresponding to such a process (with a single imaginary frequency) could be found.[46] In this work, loss of H_2 and HCN from acrylonitrile was studied via both the vinylidene and ethylidine types of pathways, as well as pathways that involve hydrogen migration followed by CC bond cleavage, which are similar to those occurring in succinonitrile. In the study of the latter mechanisms only the singlet pathways were considered.

Concerted Elimination of HCN To Form Vinylidene. There are two distinct ways in which the one-step, concerted elimination of HCN from acrylonitrile can occur, as shown in Figure 5a. The first of these corresponds to a H atom transfer to the cyanide group, with a simultaneous CC bond break, as implied by the transition state (structure **43**). In this transition state the forming CH bond was found to be quite long (1.43 Å), while the breaking CH bond was only slightly longer than the equilibrium bond length (1.120 Å). The breaking CC bond, however, was found to be 2.27 Å long, with the HCN being near-linear. The critical barrier height for this step was found to be 421 kJ mol^{-1} at 0 K, while the *A* factor and activation energies in the temperature range 1400−2100 K were calculated to be 5.9×10^{15} s^{-1} and 442 kJ mol^{-1}. The second pathway proceeds via a planar transition state (structure **44**) that results when the CN group in acrylonitrile swings toward the hydrogen atom and forms a CH bond while the CC bond breaks. However, this structure is actually a second-order saddle point, with one of the imaginary frequencies corresponding to an out-of-plane mode. Allowing structure **44** to become nonplanar did lead to a first-order saddle point, but the resulting transition state (structure **62**) connects with a different reactant, indicating the presence of another pathway, to be discussed later. The critical barrier for this pathway via structure **44** at 0 K was found to be 410 kJ mol^{-1}, with an *A* factor and activation energy in the temperature range of 1400−2100 K of 3.5×10^{13} s^{-1} and 412 kJ mol^{-1}. Consequently, this is an unimportant reaction and it is not included in the kinetic model. This first step in the decomposition reaction of acrylonitrile, resulting in HCN and vinylidine (structure **45**), was found to be 345 kJ mol^{-1} endothermic at 0 K. The following step is the well-known low-energy rearrangement of vinylidine to acetylene,[46] via a low-energy transition state (structure **46**). In this work, the barrier to decomposition, computed using G2, was found to be just 2 kJ mol^{-1} at 0 K. This result is consistent with those obtained previously.[46]

Elimination of H_2 To Form Cyanovinylidene. The concerted elimination of H_2 from acrylonitrile occurs the same way as the analogous process in ethylene,[46] but now there are two slightly different pathways corresponding to the cis or trans orientation of the departing H_2 in the transition states, as shown in Figure 5b. The geometries of the transition states (structures **47** and **48**) are very similar to that obtained for ethylene, while the computed critical energies at 0 K, viz. 406 and 401 kJ mol^{-1}, respectively, are slightly higher than in ethylene. The resulting *A* factors and activation energies in the temperature range 1400−2100 K are 1.9×10^{15} s^{-1}, 1.7×10^{15} s^{-1}, 429 kJ mol^{-1}, and 422 kJ mol^{-1}, respectively. The cyanovinylidene intermediate (structure **49**) that results can then rearrange to form cyanoacetylene, which can occur via hydrogen migration, as in vinylidene, or by a qualitatively similar migration of CN. The critical energy for the hydrogen migration, via structure **50** as transition state, was found to be 5 kJ mol^{-1}, nearly the same as in vinylidene. Migration of CN occurs via a high-energy transition state (structure **51**), which is ∼120 kJ mol^{-1} higher than the barrier to hydrogen migration. This pathway is therefore unimportant in the rearrangement process. The cyanoacetylene product (structure **52**) is a conjugated molecule and the high degree of π electron delocalization is manifested in the very short, formally single CC bond of length 1.375 Å.

Formation of 2-Cyanoethylidene. The interconversion of acrylonitrile and 2-cyanoethylidene (structure **26**) is analogous to the interconversion of ethylene and ethylidine, although depending on the relative orientation of the cyano moiety and the migrating H atom, two slightly different pathways are possible. 2-Cyanoethylidene in turn can eliminate either H_2 or HCN. The salient features of these pathways are given in Figure 5c. As for the analogous 1,2-H migration in ethylene followed

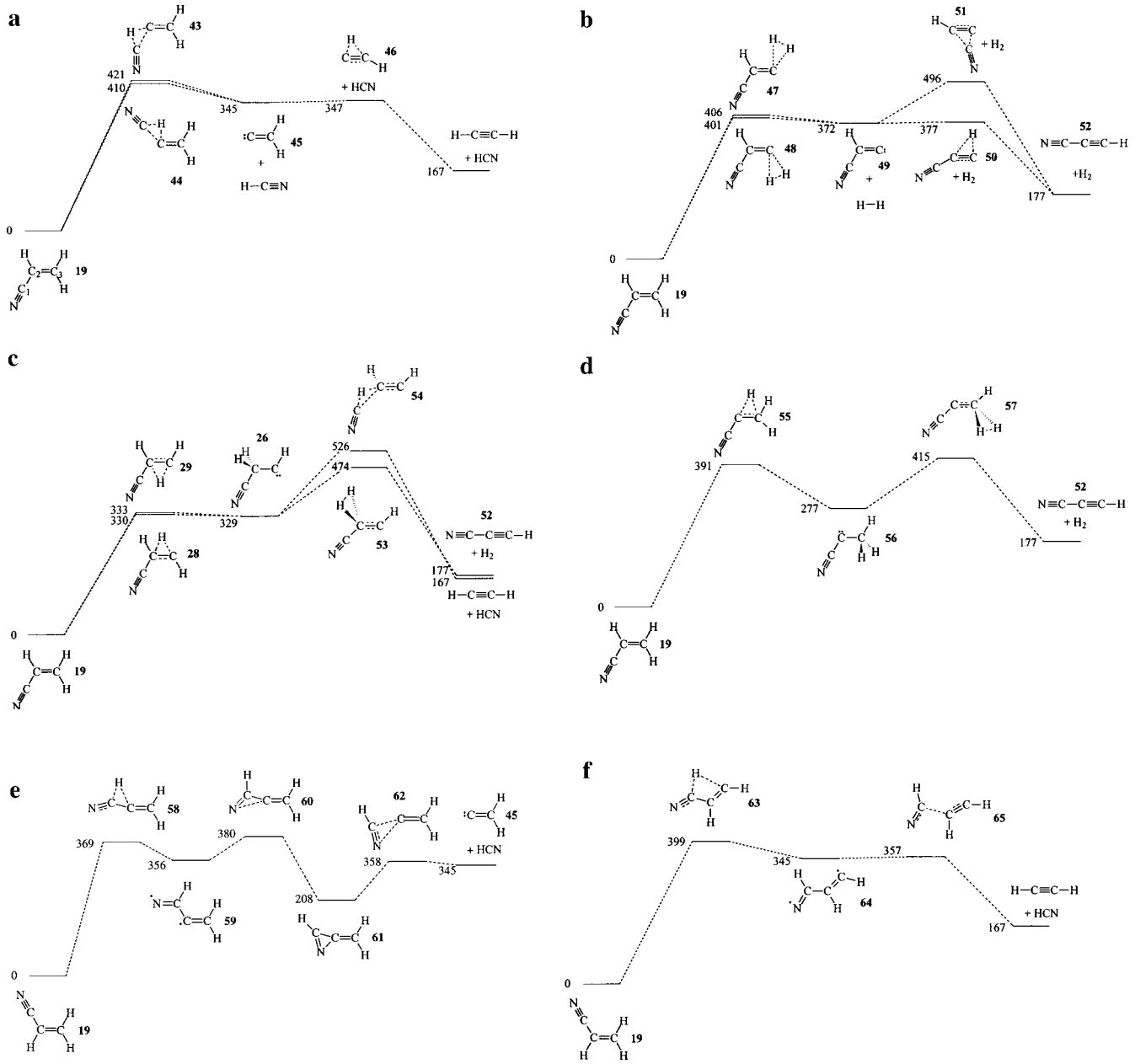

Figure 5. (a) Potential energy surface for decomposition of acrylonitrile by concerted elimination of HCN to form vinylidene. (Energies at 0 K given in kJ mol^{-1}.) (b) Potential energy surface for decomposition of acrylonitrile by elimination of H_2 to form cyanovinylidene. (Energies at 0 K given in kJ mol^{-1}.) (c) Potential energy surface for decomposition of acrylonitrile via 2-cyanoethylidene. (Energies at 0 K given in kJ mol^{-1}.) (d) Potential energy surface for decomposition of acrylonitrile via 1-cyanoethylidene. (Energies at 0 K given in kJ mol^{-1}.) (e) Potential energy surface for decomposition of acrylonitrile by nonconcerted loss of HCN via 1,2-H migration. (Energies at 0 K given in kJ mol^{-1}.) (f) Potential energy surface for decomposition of acrylonitrile by nonconcerted loss of HCN via 1,3-H migration. (Energies at 0 K given in kJ mol^{-1}.)

by 1,1-H_2 elimination, the second step is the more energetic one. The structure of the transition state leading to loss of H_2 (structure **53**) is very similar to that found in the ethylene decomposition reaction. Although the cyanoacetylene fragment in the transition state was found to be almost planar, with the CCCH dihedral angle being 13.6°, the structure is quite asymmetric, with the breaking CH bond lengths being 1.396 and 1.454 Å. The critical barrier for this process at 0 K was found to be 145 kJ mol^{-1}, while the *A* factor and activation energies in the temperature range 1400−2100 K are 4.0×10^{13} s^{-1} and 158 kJ mol^{-1} respectively. The transition state leading to the loss of HCN (structure **54**) was found to correspond to a higher critical energy, 197 kJ mol^{-1} at 0 K, with the *A* factor and activation energy in the temperature range 1400−2100 K being 1.9×10^{13} s^{-1} and 206 kJ mol^{-1}, respectively. In this structure the acetylene fragment was found to be near-planar, while the departing HCN is quite bent, the bond angle being 145.8°.

Formation of 1-Cyanoethylidene. Acrylonitrile could also form 1-cyanoethylidene (structure **56**) as an intermediate, via a process that takes place in the opposite direction to that discussed in the previous section. The PES corresponding to this pathway is summarized in Figure 5d. The transition state (structure **55**) leading to the formation of 1-cyanoethylidene has a significantly higher energy (391 kJ mol^{-1} at 0 K) than the transition state that led to 2-cyanoethylidene, even though the former carbene is the more stable isomer, by 52 kJ mol^{-1}. Thus, in contrast with the interconversion of acrylonitrile and 2-cyanoethylidene, there is now a significant barrier to the reverse reaction. The forward and reverse *A* factors and activation energies for this

process in the temperature range 1400−2100 K were found to be 9.5×10^{13} s^{-1}, 1.2×10^{13} s^{-1}, 402 kJ mol^{-1}, and 120 kJ mol^{-1}, respectively. 1-Cyanoethylidene can eliminate H_2, with the concomitant formation of cyanoacetylene. The transition state for this process (structure **57**) was found to be of C_s symmetry, with the breaking CH bonds being 1.295 Å, shorter than in the analogous H_2 elimination process from 2-cyanoethylidene. The critical barrier at 0 K for this reaction was found to be 138 kJ mol^{-1}, while the *A* factor and activation energy in the temperature range 1400−2100 K were computed to be 5.9×10^{13} s^{-1} and 150 kJ mol^{-1}, respectively.

Nonconcerted Loss of HCN via 1,2-H Migration. In this reaction pathway, summarized in Figure 5e, the first step is the formation of a biradical intermediate (structure **59**), as a result of a 1,2-H transfer. The transition state (structure **58**) as well as the reactant and product in this reaction was found to be planar, which is somewhat unusual in a 1,2-H migration. However, this reaction is somewhat unique in that all three species are conjugated and the π electron delocalization is of course optimal for planar structures. The critical energy of this reaction was found to be 369 kJ mol^{-1} at 0 K, and this step was found to be 361 kJ mol^{-1} endothermic. The energy of the biradical intermediate (structure **59**) relative to acrylonitrile was calculated at the CASPT2(10/10)/VTZ2P level of theory. The forward and reverse *A* factors and activation energies were found to be 3.7×10^{14} s^{-1}, 1.9×10^{13} s^{-1}, 385 kJ mol^{-1}, and 14 kJ mol^{-1}, respectively, in the temperature range 1400−2100 K. The biradical intermediate was found to be able to cyclize (via structure **60**) to a fairly stable, closed shell molecule (structure **61**), which then loses HCN. The transition state (structure **60**) leading to the cyclic intermediate is characterized by a very long (forming) CN bond of length ∼2.3 Å and a correspondingly large NCC angle of ∼113°. The cyclic, conjugated intermediate (structure **61**) is isoelectronic with methylene cyclopropene and its high stability can be explained in terms of the large π delocalization (resonance) energy that such a molecule is expected to possess. The geometric parameters, viz., short CC and CN "single" bonds and somewhat long CC and CN "double" bonds are consistent with the high level of π delocalization. The cyclization reaction at 0 K was calculated to be 148 kJ mol^{-1} exothermic, with a critical barrier of 24 kJ mol^{-1}. The forward and reverse *A* factors and activation energies for this step in the temperature range 1400−2100 K were found to be 5.5×10^{12} s^{-1}, 1.8×10^{14} s^{-1}, 21 kJ mol^{-1}, and 182 kJ mol^{-1}, respectively. Loss of HCN is then predicted to occur by a one-step process, via transition state **62**, whose geometry was optimized using the CASSCF method. The structure is fairly loose, with the HCN and vinylidene fragments separated by ∼2 Å, the lengths of the breaking CC and CN bonds being approximately 1.9 and 2.4 Å, respectively. As in the case of a similar bond fission reaction in succinonitrile (involving structures **22**, **24**, and **26**), the structure of this transition state is such that one may consider the possibility that it connects the biradical structure **59** as reactant with HCN and vinylidene as products on the reaction path. However, the geometry relaxations along the reaction path (when starting at the transition state) consistently converged to the cyclic structure. A more extensive search failed to locate another transition state (that would connect the biradical and the products); irrespective of the starting structures, the optimizations invariably converged to structure **62**. The critical barrier for this step at 0 K was found to be 150 kJ mol^{-1}, while the corresponding *A* factor and activation energy in the temperature range 1400−2100 K were calculated to be 2.2×10^{15} s^{-1} and 165 kJ mol^{-1}, respectively.

Nonconcerted Loss of HCN via 1,3-H Migration. 1,3-H migration in acrylonitrile, as a first step, defines another possible pathway, as shown in Figure 5f, that also leads to the elimination of HCN. This occurs via structure **63** as the transition state and results in a biradical intermediate (structure **64**). The transition state was found to be planar with CH bond lengths of 1.28 and 1.86 Å, respectively, for the forming and breaking bonds. The critical barrier for this step at 0 K was found to be 399 kJ mol^{-1}, which is 30 kJ mol^{-1} higher than the critical energy for the 1,2-H transfer discussed in the previous section. With respect to stability, the biradical intermediate (**64**) (whose energy was obtained on the basis of CASPT2(10/10)/VTZ2P calculations) is comparable with its isomer (**59**) that is an intermediate of the 1,2-H transfer step. The 1,3-H migration was found to be 345 kJ mol^{-1} endothermic at 0 K and the forward and reverse *A* factors and activation energies in the temperature range 1400−2100 K were found to be 1.4×10^{14} s^{-1}, 1.5×10^{13} s^{-1}, 414 kJ mol^{-1}, and 60 kJ mol^{-1} respectively. This biradical intermediate can readily undergo CC bond cleavage to produce HCN and acetylene. The transition state (structure **65**) for this process was found to have a breaking CC bond length of ∼1.7 Å. This step was found to have a critical barrier of 9 kJ mol^{-1} at 0 K, while the corresponding *A* factor and activation energy in the temperature range 1400−2100 K were found to be 4.0×10^{14} s^{-1} and 22 kJ mol^{-1} respectively.

Summary of Computational Results. The key reactions studied in this work by ab initio methods are the decomposition of acetonitrile to yield cyanomethyl and H, the subsequent reaction between H and acetonitrile (leading to the products CH_3 and HCN), the recombination of cyanomethyls to form succinonitrile, the decomposition of the latter to yield acrylonitrile and HCN, and finally, the decomposition reactions of acrylonitrile to acetylene and HCN and to cyanoacetylene and H_2, respectively.

A crucial aspect of the work has been the ab initio computation of the heat of formation of cyanomethyl as the accuracy of the kinetic model critically depends on this quantity. The reaction between H and acetonitrile are similarly an important part of the kinetic model and the ab initio parameters are used in the model without any adjustment.

Six distinct intramolecular reaction pathways were considered in the study of the decomposition of succinonitrile, although only four of these (1,3-H transfer, 1,2-H transfer, rearrangement to isocyanide, and CH bond fission) were found to be sufficiently important to be included in the kinetic model. The most important of these is the CH bond fission reaction, viz., H loss, which is the dominant pathway at the higher temperatures. The bimolecular reaction between H and succinonitrile, where H effectively plays the role of a catalyst, is included in the model, although it is not a sensitive reaction. As discussed in the next section, H abstraction by cyanomethyl is the most important reaction at the lower temperatures that leads to the formation of acrylonitrile and HCN.

Concerning the decomposition of acrylonitrile, six distinct mechanisms were studied. These are concerted 1,1-elimination of HCN or of H_2 (resulting in acetylene and HCN and cyanoacetylene and H_2, respectively), 1,2-H migrations (to form two cyanoethylidene isomers that decompose to acetylene and HCN and cyanoacetylene and H_2), and nonconcerted HCN loss reactions via 1,2-H and 1,3-H migrations. The computed critical energies for these pathways were found to be too high, however, by ∼12 and ∼36 kJ mol^{-1} for the HCN and H_2 elimination reactions, respectively, to successfully model the decomposition of acrylonitrile. As discussed in the next section, the rate

TABLE 3: Thermochemical Parameters for the Acetonitrile System

	$\Delta_f H^0_{298}$/kJ mol^{-1}	S^0_{298}/J K^{-1} mol^{-1}	C_p^0/J K^{-1} mol^{-1}					ref
			300	500	1000	1500	2000	
CH_3CN	73.9	244.8	52.4	69.4	98.3	112.3	120.6	36[b]
CH_2CN	263.4	250.6	54.5	67.7	86.2	95.4	100.0	PW/abin[c]
SUCC[a]	198.6	328.9	98.0	131.1	178.5	200.4	211.0	PW/abin[c]
ISUCC[a]	272.6	331.3	93.4	127.3	178.2	201.7	213.1	PW/abin[c]
$NCCHCH_2CN$	381.8	337.0	95.9	125.8	166.5	184.6	193.4	PW/abin[c]
H_2CCHCN	183.5	272.9	63.8	87.6	120.9	136.6	144.5	63[b]
CH_2CH_2CN	245.4	286.7	71.7	97.2	136.9	156.9	165.6	PW/add[d]
$C_4H_2N_2$	338.7	299.9	84.7	112.8	147.9	163.0	170.5	PW/add
HCCHCN	409.5	280.5	66.6	83.0	105.8	116.2	122.7	7/add
HCCCN	380.6	236.2	64.8	78.1	93.7	101.4	105.4	64/abin
CH_3CHCN	226.7	290.8	64.8	90.8	133.5	154.3	165.2	PW/add
NCCH(3)	480.2	234.2	46.1	55.1	66.4	71.6	74.3	65/abin
C_2N	604.7	239.0	44.6	50.2	57.5	59.8	61.2	66

[a] Name as given in Table 2. [b] S^0_{298} and C_p^0 values calculated statistically in the present work. [c] Evaluated by ab initio calculation in the present work. [d] Estimated by group additivity methods in the present work.

parameters for these reactions, viz., (28) and (29), were instead derived on the basis of experimental data.[2]

Kinetic Modeling. Kinetic modeling using the model given in Table 2 was performed using the Sandia CHEMKIN code,[47] together with the shock tube code[48] (modified to allow for cooling by the reflected rarefaction wave) and the ordinary differential equation solver LSODE.[49] Predicted decomposition and product profiles are compared with experimental data in Figure 1. Rate sensitivity analysis has been carried out on the model using the SENKIN[50] code. Thermodynamic sensitivity analysis was performed using the code HSENKIN developed by Muris and Haynes.[51] Several of the key rate constants in the model have been evaluated as discussed above from ab initio calculations. In general, reverse rate constants have been evaluated using the equilibrium constants, which, in turn, have been calculated from the thermochemistry by standard methods. Thermochemical parameters for species important in the acetonitrile system are given in Table 3. For comparison purposes, the reverse rate constants given in Table 2 have been fitted to the simple Arrhenius form over the temperature range of 1400−2100 K.

In addition to reactions described above, there are bimolecular reactions, including abstraction, addition, and recombination reactions whose rate constants in some cases have been estimated by comparison with analogous reactions of known rate constant. In general, reactions for which rate constants have been estimated are not sensitive reactions in the model. The model contains a subset of C_1, C_2, and some C_3 and C_4 species reactions whose rate constants have been taken from the GRIMech,[52] Warnatz,[53] and Miller and Bowman[54] compilations. At temperatures around 2000 K, the C−C bond fission reaction (23) of acetonitrile shows some sensitivity and the model contains an estimated rate constant k_{23}. This value, which is specific to our pressure regime, was chosen to optimize agreement between experimental and theoretical acetonitrile profiles above 2000 K. Also in this temperature region we have included decomposition reactions of CH_2CN radicals to produce both CCN and triplet state NCCH(3) species. Rate constants for these reactions, which would be expected to be in the falloff regime, were estimated by RRKM methods (using program UNIMOL) and the values of k_{72} and k_{73} thus obtained are specific to our pressure of 12 atm. Apart from the metathesis reaction (86) between CN and CH_2CN radicals, which produces NCCH(3), none of the reactions involving CCN or NCCH(3) is a sensitive reaction. Also, a direct chemiactivated reaction between two CH_2CN radicals to form HCN and acrylonitrile, reaction 8, was included with rate parameters obtained by the use of QRRK analysis, taking into account the barriers derived by ab initio calculations as described above.

Comparison between the predictions of the kinetic model and experiment is made in Figure 1. It may be seen that the model gives an acceptable fit to the experimental species yields. The model also predicts that only an indetectably low yield of succinonitrile is formed at all temperatures. Rate sensitivity analysis of the model shows that overwhelmingly the most sensitive reaction for overall reaction rate and for all major species is the initiation reaction 1. Initially, we used our experimental value of k_{dis} for k_1. On account of the high sensitivity of virtually all product species to k_1 throughout the entire temperature range, we have made minor changes to our initially chosen value of k_1 to best fit the product profiles. The adjustment to k_1 is within our experimental error but probably reflects the contribution of secondary reactions to the disappearance of acetonitrile. The value of k_1 given in Table 2 is specific to our pressures (∼12 atm). Reaction 2, the addition of H and subsequent fission of HCN exhibits considerable sensitivity for the overall reaction and for major products. Rate sensitivity coefficients of the most sensitive reactions for the major products are shown in Figure 6.

The high-temperature tail of the acetonitrile profile agreed less well with experiment when the literature value for $\Delta_f H^0_{298}$ (CH_2CN) of 245 kJ mol^{-1} was used. Thermodynamic sensitivity analysis (using HSENKIN) indicated that an increase in the enthalpy of formation of this species would bring modeled and experimental profiles into better agreement. The optimal agreement occurred for $\Delta_f H^0_{298}$ (CH_2CN) = 263 ± 9 kJ mol^{-1}, in excellent agreement with the ab initio result.

As can be seen in Figure 1, both acrylonitrile and cyanoacetylene exhibit maxima in their yields at temperatures around 1700 K. Kinetic modeling of these profiles is a challenge. In the initial formulation of the kinetic model we adopted the ab initio barriers for 1,1 elimination of H_2 and HCN from acrylonitrile and assumed a similar barrier for 1,1 elimination of HCN from the fumaronitriles (reactions 28, 29, and 82, respectively). These are all sensitive reactions, at least for formation of acrylonitrile and cyanoacetylene. However, the ab initio barriers gave rise to rate constants for these reactions that were too small and led to calculated yields of these products that were too low in comparison with experiment, and also led to a high residual yield of fumaronitriles.

As argued in the previous section, the transition state for 1,1 elimination of H_2 from acrylonitrile should be analogous to the 1,1 elimination from ethylene. Some years ago, Kiefer et al.[55]

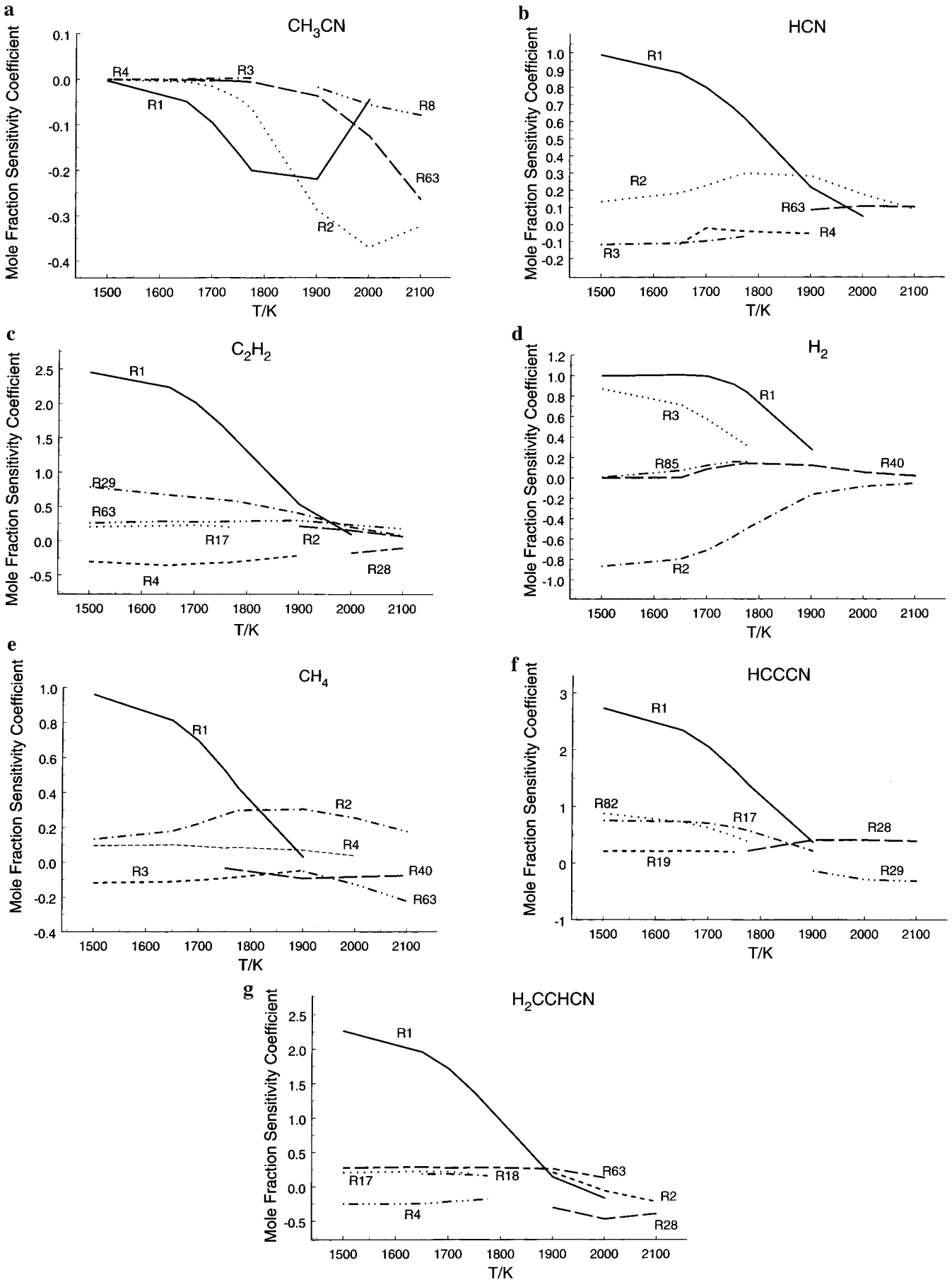

Figure 6. Variation with temperature of sensitivity coefficients for the designated species. Only the most sensitive reactions are shown. Reaction numbers are as given in Table 2.

carried out a RRKM extrapolation of kinetic data for ethylene pyrolysis measured by three different laboratories, all at pressures just above the low-pressure limit. All sets of data extrapolated to a critical energy for 1,1 elimination of H_2 from ethylene of 356 ± 8 kJ mol^{-1}. This is some 36 kJ lower in energy than the ab initio barrier height obtained by Jensen et al.,[46] which in turn agrees closely with our G2 result as well as the earlier value of Raghavachari et al.[56] We have now extrapolated some unpublished kinetic data for ethylene decomposition measured by Organ[57] in this laboratory using two techniques—single pulse shock tube product analysis and infrared real time laser absorption spectroscopy of C_2H_4 behind reflected shocks, both studies at a pressure of 22 atm, just below the high-pressure limit. Using the same RRKM parameters as Kiefer et al.,[55] our RRKM extrapolation leads to the same critical energy of 356 ± 8 kJ mol^{-1}. There is clearly an anomaly between the RRKM extrapolated result and the ab initio calculation that we are unable to reconcile at present.

We therefore believe that the same anomaly exists for the analogous 1,1 eliminations from acrylonitrile and the fumaronitriles. Therefore, to model our acrylonitrile and cyanoacetylene data we first adopted the experimental values given by Lifshitz et al.[2] for a pressure of 3 atm and made an RRKM extrapolation to our average pressure of 12 atm. However, the values of k_{28}, k_{29}, and k_{82} so evaluated were too large so that we have adjusted the respective activation energies to best fit our profiles of cyanoacetylene and acrylonitrile. The rate constants k_{28}, k_{29}, and k_{82} as shown in Table 2 are specific to our pressure of 12 atm and are comparable with the literature values[52] for the analogous elimination of H_2 from ethylene. It should be pointed out that, at 1700 K, the model predicts that the rate constant for decomposition of acrylonitrile must be about 10^3 s^{-1} to model the experimental profiles of acrylonitrile and cyanoacetylene correctly. Summing all the elimination paths we have identified above that produce H_2 from acrylonitrile results in an overall rate constant of ∼300 s^{-1} at 1700 K, while the rate constant for the elimination of HCN is ∼500 s^{-1}. Thus the discrepancy between theory and model rate constants could be resolved if it is assumed that the former overestimated the elimination barriers by about 12 kJ mol^{-1}. Such a discrepancy is only about twice as large as the expected average deviation between G2 and experiment, when G2 is applied to the prediction of dissociation energies, ionization energies, electron affinities, and proton affinities.[58] In the absence of comparable systematic studies on the performance of G2 when applied to the computation of critical energy barriers, an error of 12 kJ mol^{-1} may well be judged as acceptable and does not necessarily imply major shortcomings in the kinetic model or the theoretical methodology employed. Unfortunately, the same cannot be said of the 1,1 elimination reaction in ethylene. A discrepancy of 36 kJ mol^{-1} in the critical energy appears to be too large to be explained as due to the neglect of quantum mechanical tunneling. Nevertheless, so as to be able to quantify its contributions to the rate of H_2 elimination, we have undertaken a theoretical study of tunneling in this system (treating it as a two-dimensional system, where the two degrees of freedom effectively correspond to the motion of the hydrogens relative to vinylidene, given the appropriate two-dimensional PES).

The model predicts a maximum yield of succinonitrile of 1.1% (based on the initial reactant) at a temperature of 1625 K. This low yield, together with the low volatility of succinonitrile (BP 267 °C), would render it most unlikely to be detected in the shock tube experiments. At 1625 K and at the end of the residence time (885 μs) just prior to the rarefaction wave quenching, the reaction flux forming succinonitrile is 2.0×10^{-5} mol cm^{-3} s^{-1}, arising from reaction 7, the recombination of two CH_2CN radicals. The net reaction flux decomposing succinonitrile is also 2.0×10^{-5} mol cm^{-3} s^{-1}, of which 90% takes place via reaction 17, abstraction from succinonitrile by CH_2CN. The 1,3-H transfer pathway (reaction 9) accounts for 3.0% of reaction flux. The remainder of the reaction flux comprises the bimolecular reactions (13), (14), and (15) together with the 1,2-H transfer pathway on the singlet surface (reaction 78), each of these four reactions contributing approximately equally to decomposition of succinonitrile. Although the barrier to isomerization of succinonitrile is the lowest of all the rearrangements of this molecule, there is a negligible decomposition flux passing through reactions 10 and 11. In essence, succinonitrile and its isocyanide equilibrate rapidly but the barrier for decomposition of the latter is too large. In the rarefaction wave, recombination of CH_2CN radicals will continue whereas the destruction reactions will be essentially frozen because of their appreciable activation energies.

At temperatures above about 1800 K, decomposition of succinonitrile is rapid and the model predicts a negligible yield of this intermediate. At these higher temperatures the H fission reaction (12) becomes an important mode of destruction of succinonitrile.

Concerning the formation of acrylonitrile and cyanoacetylene, the maximum yields of these occur at ∼1700 and ∼1750 K, respectively. Of the total reaction flux forming H_2CCHCN, 42% results from reaction 18, loss of CN from the radical produced from succinonitrile by H loss. About 22% comes from the reverse of reaction 58, i.e., H fission from CH_3CHCN, which is in turn produced by H loss from ethyl cyanide. The remaining formation flux comes approximately equally from reaction 8 (the direct chemiactivated reaction between two CH_2CN radicals), reaction 9 (the 1,3-H transfer reaction of succinonitrile), H loss from the CH_2CH_2CN radical from ethyl cyanide, and reaction 79 involving the cyclic intermediate identified on the singlet potential surface for 1,2-H transfer in succinonitrile. At 1700 K there is a small decomposition flux from acrylonitrile. This takes place principally via reactions 28 and 29 which are the 1,1 elimination reactions of acrylonitrile to produce HCCCN + H_2 and C_2H_2 + HCN, respectively.

At 1700 K, nearly all reaction flux involving HCCCN leads to its formation. About 85% of flux is via reaction 82, the 1,1 elimination of HCN from the fumaronitriles. Reaction 28 contributes about 12%. Thus, both acrylonitrile and cyanoacetylene originate largely from succinonitrile, albeit indirectly in the case of the latter product, although ethyl cyanide is also a precursor of the former product.

We now turn to a consideration of a falloff calculation of the rate constant for fission of a hydrogen from acetonitrile (reaction 1). Using the ab initio CASSCF geometry and (unscaled) frequencies of acetonitrile and the transition state with the ab initio value of the CH bond distance of 2.532 Å in the transition state as calculated according to Variational Transition State Theory, together with the critical energy of 388 kJ mol^{-1} (calculated at the G2 level of theory), we have carried out a RRKM high-pressure limit calculation of k_1. Over the temperature range of 1350−1750 K, the Arrhenius form $k_{1\infty} = 1.2 \times 10^{16} \exp(-413 \text{ kJ mol}^{-1}/RT)$ s^{-1} holds well, although the empirical expression $9.18 \times 10^{12} T^{0.85} \exp(-401 \text{ kJ mol}^{-1}/RT)$ gives an even better fit of the RRKM results. Our value of $k_1 = 8 \times 10^{14} \exp(-397 \text{ kJ mol}^{-1}/RT)$ for an average pressure of 12 atm was evaluated from CH_3CN profiles over the temperature range of 1500−1750 K. Using a value of $\langle \Delta E_{\text{down}} \rangle$

of 800 cm^{-1} and the calculated $k_{1\infty}$ and critical energy, we can substantially reproduce our 12 atm kinetic results by means of an RRKM falloff calculation.

Lifshitz et al.[2] obtained a value for k_1 of 6.17×10^{15} exp(−404 kJ mol^{-1}/RT) s^{-1} from CH_3CN profiles over the somewhat lower temperature range of 1350−1550 K at about 3 atm pressure. Their values of k_1 are, within experimental error, equal to the calculated high-pressure limit values over their range of temperatures. For their slightly lower temperature range, it might be expected that their rates would be somewhat less affected by falloff. We have not, however, been able to reproduce their result with a value of $\langle \Delta E_{down} \rangle$ of 800 cm^{-1} or, indeed, with a very much larger value of this parameter. We cannot explain this discrepancy since we would expect that a molecule as small as acetonitrile dilute in an argon bath gas at pressures around 3 atm should show significant falloff in its fission reaction.

In their recent modeling study, Lifshitz and Tamburu[5] report the value of $k_1 = 1.0 \times 10^{15}$ exp(−389 kJ mol^{-1}/RT) s^{-1}, presumably for a pressure of 3 atm. This value, derived from their ignition delay studies,[4] is, at 1500 K, lower than their earlier one by about a factor of 2 but is still about a factor of 2 larger than ours at the same temperature.

Turning to a comparison between our kinetic models for acetonitrile pyrolysis, both models agree that the major route to primary products HCN, H_2, and CH_4 involves initiation by CH fission, H addition and fission to CH_3 + HCN, and H and CH_3 abstraction reactions to form hydrogen and methane (reactions 1−4, Table 2) with minor differences between models in the rate constants for these reactions. The major difference between the models lies in the fate of the $C_4H_4N_2$ species arising from recombination of two CH_2CN radicals. We have identified this recombination product as succinonitrile, and our detailed study of its reaction potential energy surface has enabled a better understanding of the mechanism of its subsequent decomposition pathways and of the formation of acrylonitrile and cyanoacetylene to be made. Lifshitz and Tamburu considered that the major decomposition pathways of $C_4H_4N_2$ were to form H_2CCHCN + HCN or C_2N_2 + C_2H_4. As discussed above, at high temperatures, our ab initio studies show that H fission from succinonitrile is a most important route at high temperatures and we find no evidence for a route to cyanogen.

Conclusions

The pyrolysis of acetonitrile over the temperature range of 1500−2100 K can be simulated by an 87 step reaction kinetic model. The pyrolysis is initiated via hydrogen fission to form the cyanomethyl, CH_2CN, radical. Extensive ab initio quantum chemical calculations on the C_2H_2N potential energy surface located five isomers of which the lowest lying is cyanomethyl. On the basis of isodesmic reactions calculated at the G2 level of theory, the value of $\Delta_f H^0_{298}$ (CH_2CN) was found to be 263 ± 9 kJ mol^{-1}, about 20 kJ mol^{-1} higher than previously reported. In the reaction model the initiation rate constant is overwhelmingly the most sensitive for overall reaction and for all products of significance. The limiting high-pressure value for this rate constant of $k_{1\infty} = 1.2 \times 10^{16}$ exp(−413 kJ mol^{-1}/RT) s^{-1} obtained by ab initio variational transition state calculation agrees with our extrapolated experimental measurement for an average pressure of 12 atm. The major nitrogen-containing product is HCN, arising from H addition and subsequent fission of the adduct. Rate constants for the addition and fission reaction have been derived by ab initio calculation.

Recombination of two CH_2CN radicals leads to the formation of succinonitrile as an intermediate. The nonobservation of this product in shock tube experiments is attributed to its low calculated yield (max. ~1% based on initial reactant). This, together with its low volatility, precludes its observation among the products of a single pulse shock tube. Succinonitrile has, however, been detected in trace quantities in the products from a completely stirred flow reactor. A detailed ab initio study of the succinonitrile potential energy surface has been made to search for possible intramolecular decomposition pathways of low barrier to acrylonitrile and HCN. However, succinonitrile decomposes principally via hydrogen loss. At the lower temperatures of this study, this takes place by H-abstraction by cyanomethyl. At higher temperatures, direct fission becomes an important route. The $NCCHCH_2CN$ radical so produced is an important precursor of acrylonitrile but also leads to the intermediate formation of the fumaronitriles, which, in turn, are important for cyanoacetylene formation. Rate constants for these reactions have been evaluated by ab initio calculation. Ethyl cyanide is also a source of acrylonitrile. Several H_2 and HCN elimination pathways from acrylonitrile have been identified.

Acknowledgment. The financial support of the Australian Research Council is acknowledged. K.S. gratefully acknowledges the award of an Australian Postgraduate Research Scholarship.

Supporting Information Available: Geometries and energies of all molecular species discussed in this work are available in Tables 1S−9S. This information is available free of charge via the Internet at http://pubs.acs.org.

References and Notes

(1) Bowman, C. T. *24th International Symposium on Combustion;* The Combustion Institute: Pittsburgh, PA, 1992; p 859.
(2) Lifshitz, A.; Moran, A.; Bidani, S. *Int. J. Chem. Kinet.* **1987**, *19*, 61.
(3) Ikeda, E.; Mackie, J. C. *26th International Symposium on Combustion;* The Combustion Institute: Pittsburgh, PA, 1996; p 597.
(4) Lifshitz, A.; Tamburu, C.; Carroll, H. F. *Int. J. Chem. Kinet.* **1997**, *29*, 839.
(5) Lifshitz, A.; Tamburu, C. *Int. J. Chem. Kinet.* **1998**, *30*, 341.
(6) Mackie, J. C.; Colket, M. B.; Nelson, P. F.; Esler, M. *Int. J. Chem. Kinet.* **1991**, *23*, 733.
(7) Doughty, A.; Mackie, J. C. *J. Phys. Chem.* **1992**, *96*, 272.
(8) Ikeda, E.; Mackie, J. C. *J. Anal. Appl. Pyrol.* **1995**, *34*, 47.
(9) Ikeda, E. B. Sc. (Hons.) Thesis, University of Sydney, 1993.
(10) Curtiss, L. A.; Raghavachari, K.; Trucks, G. W.; Pople, J. A. *J. Chem. Phys.* **1991**, *94*, 7221.
(11) Roos, B. O.; Taylor, P. R.; Siegbahn, P. E. S. *Chem. Phys.* **1980**, *48*, 157.
(12) Roos, B. O. In *Ab initio Methods in Quantum Chemistry*; Lawley, K. P., Ed.; Wiley: Chichester, U.K., 1987; Vol. II, p 399.
(13) Dunning, T. H. *J. Chem. Phys.* **1970**, *53*, 2823.
(14) Andersson, K.; Malmqvist, P.-Å.; Roos, B. O.; Sadlej, A. J.; Wolinski, K. *J. Chem. Phys.* **1990**, *94*, 5483.
(15) Andersson, K.; Malmqvist, P.-Å.; Roos, B. O. *J. Chem. Phys.* **1992**, *96*, 1282.
(16) Dunning, T. H. *J. Chem. Phys.* **1987**, *90*, 1007.
(17) Woon, D. E.; Dunning, T. H. *J. Chem. Phys.* **1990**, *98*, 1358.
(18) Steinfeld, J. I.; Francisco, J. S.; Hase, W. L. *Chemical Kinetics and Dynamics*; Prentice Hall: Englewood Cliffs, NJ, 1989; p 308.
(19) McQuarrie, D. A. *Statistical Mechanics*; Harper & Row: New York, 1973; p 129.
(20) Nordholm, S.; Bacskay, G. *Chem. Phys. Lett.* **1976**, *42*, 253.
(21) Hase, W. L.; Mondro, S. L.; Duchovic, R. J.; Hirst, D. M. *J. Am. Chem. Soc.* **1987**, *109*, 2916.
(22) Gilbert, R. G.; Smith, S. C.; Jordan, M. T. UNIMOL Program Suite (Calculation of Falloff Curves for Unimolecular and Recombination Reactions), 1993. Available from the authors: School of Chemistry, University of Sydney, NSW 2006, Australia.
(23) Dean, A. M. *J. Phys. Chem.* **1985**, *89*, 4600.
(24) Westmoreland, P. R.; Howard, J. B.; Longwell, J. P.; Dean, A. M. *AIChE J.* **1986**, *32*, 1971.

(25) Frisch, M. J.; Trucks, G. W.; Head-Gordon, M.; Gill, P. M. W.; Wong, M. W.; Foresman, J. B.; Johnson, B. G.; Schlegel, H. B.; Robb, M. A.; Replogle, E. S.; Gomperts, R.; Andres, J.; Rachavachari, L. K.; Binkley, J. S.; Gonzalez, C.; Martin, R. L.; Fox, D. J.; Defrees, D. J.; Baker, J.; Stewart, J. J. P.; Pople, J. A. Gaussian 92, Revision A; Gaussian, Inc.: Pittsburgh, PA, 1992.

(26) Frisch, M. J.; Trucks, G. W.; Schlegel, H. B.; Gill, P. M. W.; Johnson, B. G.; Robb, M. A.; Cheeseman, J. R.; Keith, T.; Peterson, G. A.; Montgomery, J. A.; Raghavachari, K.; Al-Laham, M. A.; Zakrzewski, V. G.; Ortiz, J. V.; Foresman, J. B.; Cioslowski, J.; Stefanov, B. B.; Nanayakkara, A.; Challacombe, M.; Peng, C. Y.; Ayala, P. Y.; Chen, W.; Wong, M. W.; Andres, J. L.; Replogle, E. S.; Gomperts, R.; Martin, R. L.; Fox, D. J.; Binkley, J. S.; Defrees, D. J.; Baker, J.; Stewart, J. P.; Head-Gordon, M.; Gonzales, C.; Pople, J. A. GAUSSIAN94, Revision E2; Gaussian, Inc.: Pittsburgh, PA, 1994.

(27) Amos, R. D.; Rice, J. E. CADPAC 5.2: The Cambridge Analytic Derivatives Package; University of Cambridge: Cambridge, U.K., 1992.

(28) CADPAC 6.0: The Cambridge Analytical Derivatives Package Issue 6; University of Cambridge: Cambridge, U.K., 1995. A suite of quantum chemistry programs developed by R. D. Amos with contributions from I. L. Alberts, J. S. Andrews, S. M. Colwell, N. C. Handy, D. Jayatilaka, P. J. Knowles, R. Kobayashi, K. E. Laidig, G. Laming, A. M. Lee, P. E. Maslen, C. W. Murray, J. E. Rice, E. D. Simandiras, A. J. Stone, M.-D. Su, and D. J. Tozer.

(29) SIRIUS is an MCSCF program written by H. J. Å. Jensen, H. Agren, and J. Olsen.

(30) ABACUS is an MCSCF energy derivatives program written by T. Helgaker, H. J. Å. Jensen, P. Jorgensen, J. Olsen, and P. R. Taylor.

(31) DALTON Release 1.0 1997 is an ab initio electronic structure program, written by T. Helgaker, H. J. Å. Jensen, P. Jørgensen, J. Olsen, K. Ruud, H. Ågren, T. Anderson, K. L. Bak, V. Bakken, O. Christiansen, P. Dahle, E. K. Dalskov, T. Enevoldsen, B. Fernandez, H. Heiberg, H. Hettema, D. Jonsson, S. Kirpekar, R. Kobayashi, H. Koch, K. V. Mikkelsen, P. Norman, M. J. Packer, T. Saue, P. R. Taylor, and O. Vahtras.

(32) Andersson, K.; Blomberg, M. R. A.; Fülscher, M. P.; Kellö, V.; Lindh, R.; Malmqvist, P.-Å.; Noga, J.; Olsen, J.; Roos, B. O.; Sadlej, A. J.; Siegbahn, P. E. M.; Urban, M.; Widmark, P.-O. MOLCAS version 2; University of Lund: Lund, Sweden, 1991.

(33) Andersson, K.; Blomberg, M. R. A.; Fülscher, M. P.; Karlström, G.; Lindh, R.; Malmqvist, P.-Å.; Neogrády, P.; Olsen, J.; Roos, B. O.; Sadlej, A. J.; Schütz, M.; Seijo, L.; Serrano-Andrés, L.; Siegbahn, P. E. M.; P.-O. Widmark, P.-O. MOLCAS Version 4; Lund University: Lund, Sweden, 1997.

(34) MOLPRO is a package of ab initio programs written by H.-J. Werner and P. J. Knowles, with contributions from J. Almlöf, R. D. Amos, M. J. O. Deegan, S. T. Elbert, C. Hampel, W. Meyer, K. Peterson, R. Pitzer, A. J. Stone, P. R. Taylor, R. Lindh, M. E. Mura, and T. Thorsteinsson.

(35) Kee, R. J.; Rupley, F. M.; Miller, J. A. *The Chemkin Thermodynamic Data Base*; Sandia Report SAND87-8215; Sandia National Laboratories: Los Alamos, NM, 1987.

(36) An, X.-W.; Mansson, M. *J. Chem. Thermodyn.* **1983**, *15*, 287.

(37) King, K. D.; Goddard, R. D. *Int. J. Chem. Kinet.* **1975**, *7*, 837.

(38) Berkowitz, J.; Ellison, G. B.; Gutman, D. *J. Phys. Chem.* **1994**, *98*, 2744.

(39) Moran, S.; Ellis, H. B., Jr.; DeFrees, D. J.; McLean, A. D.; Ellison, G. B. *J. Am. Chem. Soc.* **1987**, *109*, 5996.

(40) Holmes, J. L.; Mayer, P. M. *J. Phys. Chem.* **1995**, *99*, 1366.

(41) Hehre, W. J.; Radom, L.; von R. Schleyer, P.; Pople, J. A. *Ab Initio Molecular Orbital Theory*; Wiley: New York, 1986; p 156.

(42) Doughty, A.; Mackie, J. C.; Bacskay, G. B. *J. Phys. Chem.* **1994**, *98*, 13546.

(43) Swanton, D. J.; Bacskay, G. B.; Willett, G. D.; Hush, N. S. *J. Mol. Struct. (THEOCHEM)* **1983**, *91*, 313.

(44) Mayer, P. M.; Taylor, M. S.; Wong, M. W.; Radom, L. *J. Phys. Chem. A* **1998**, *102*, 7074.

(45) Bernardi, F.; Robb, M.; Schlegel, H. B.; Tonachini, G. *J. Am. Chem. Soc.* **1984**, *106*, 1198.

(46) Jensen, J. H.; Morokuma, K.; Gordon, M. S. *J. Chem. Phys.* **1994**, *100*, 1981, and references therein.

(47) Kee, R. J.; Miller, J. A.; Jefferson, T. H. CHEMKIN: A General Purpose, Problem Independent, Transportable FORTRAN Chemical Kinetics Code Package. SANDIA National Laboratories Report SAND80-003; Sandia National Laboratories: Los Alamos, NM March 1980.

(48) Mitchell, R. D.; Kee, R. J. A General Purpose Computer Code for Predicting Chemical Kinetic Behavior behind Incident and Reflected Shocks. SANDIA National Laboratories Report SAND82-8205; Sandia National Laboratories: Los Alamos, NM March 1982.

(49) Hindmarsh, A. C. LSODE and LSODI: Two New Initial Value Differential Equation Solvers. *ACM Signum Newslett.* **1980**, *15*, 4.

(50) Lutz, A. E.; Kee, R. J.; Miller, J. A. SENKIN: A FORTRAN Program for Predicting Homogeneous Gas-Phase Chemical Kinetics with Sensitivity Analysis. SANDIA National Laboratories Report SAND87-8248; Sandia National Laboratories: Los Alamos, NM 1988.

(51) Muris, S.; Haynes, B. S. HSENKIN, Department of Chemical Engineering, University of Sydney, NSW 2006, Australia.

(52) Bowman, C. T.; Hanson, R. K.; Davidson, D. F., Gardiner, W. C.; Lissianski, V.; Smith, G. P.; Golden, D. M.; Frenklach, M.; Goldenberg, M. http://www.me.berkeley.edu/gri_mech.

(53) Warnatz, J. In *Combustion Chemistry*; Gardiner, W. C., Jr., Ed.; Springer: New York, 1984; p 197.

(54) Miller, J. A.; Bowman, C. T. *Prog. Energy Combust. Sci.* **1989**, *15*, 287.

(55) Kiefer, J. H.; Sidhu, S. S.; Kumaran, S. S.; Irdam, E. A. *Chem. Phys. Lett.* **1989**, *159*, 32.

(56) Raghavachari, K.; Frisch, M. J.; Pople, J. A.; Schleyer, P. von R. *Chem. Phys. Lett.* **1982**, *85*, 145.

(57) Organ, P. P. Ph.D. Thesis, University of Sydney, 1989.

(58) Curtiss, L. A.; Carpenter, J. E.; Raghavachari, K.; Pople, J. A. *J. Chem. Phys.* **1992**, *96*, 9030.

(59) Kiefer, J. H.; Mitchell, K. I.; Kern, R. D.; Yong, J. N. *J. Phys. Chem.* **1988**, *92*, 677.

(60) Weisssman, M. A.; Benson, S. W. *J. Phys. Chem.* **1988**, *92*, 4080.

(61) Payne, W. A.; Stief, L. J. *J. Chem. Phys.* **1976**, *64*, 1150.

(62) Mallard, W. G.; Westley, F.; Herron, J. T.; Hampson, R. G.; Frizzell, D. H. NIST Chemical Kinetic Database, Version 6.0; National Institute of Standards and Technology: Gaithersburg, MD, 1994.

(63) Halverson, F.; Stamm, R. F.; Whalen, J. J. *J. Chem. Phys.* **1948**, *16*, 808.

(64) Francisco, J. S.; Richardson, S. L. *J. Chem. Phys.* **1994**, *101*, 7707.

(65) Francisco, J. S. *Chem. Phys. Lett.* **1994**, *230*, 372.

(66) Burcat, A.; McBride, B. 1994 Ideal Gas Thermodynamic Data for Combustion and Air Pollution Use. Technion Aerospace Eng. Rep. No. 697; Technion University: Haifa, Israel Dec 1993.